ERROR CONTROL FOR *hp*-ADAPTIVE APPROXIMATIONS OF SEMI-DEFINITE EIGENVALUE PROBLEMS

STEFANO GIANI, LUKA GRUBIŠIĆ, AND JEFFREY S. OVALL

Abstract. We present reliable a-posteriori error estimates for *hp*-adaptive finite element approximations of semi-definite eigenvalue/eigenvector problems. Our model problems are motivated by the applications in photonic crystal eigenvalue computations. We present detailed numerical experiments confirming our theory and give several benchmark results which could serve the purpose of numerical testing of other adaptive procedures.

1. Introduction

Accurate computation of eigenvalues of elliptic differential operators remains a highly challenging numerical task regardless of the considerable research effort which has been recently invested in it. For operators for which particular solutions of (local) eigenvalue problems are known explicitly, a modified *method of particular solutions* such as that described [11] seems to be the most efficient means to deliver as many accurate digits in computed eigenvalues as possible. However, the class of operators to which this method can be successfully applied is limited, and does not include many operators having discontinuous or anisotropic coefficients on the highest-order derivatives (cf. [15]). For this broader class of problems, *hp*-adaptive discontinuous Galerkin (DG) methods currently appear to be the most efficient, as measured by flops per accurate digit delivered, to compute the eigenvalues/eigenvectors, see [18] and the references therein. In the present work, we put forth an *hp*-adaptive continuous Galerkin method which aims at similar practical efficiency, while supplying a much more robust error estimation theory for eigenvalue and invariant subspace computations.

The difficulty which is associated with eigenvalue/eigenvector problems for differential operators with discontinuous coefficients partly stems from the nonlinear nature of the eigenvalue problem itself and partly from the inherent singularities which the eigenvectors can posses. For instance it is known that eigenvectors of such operators can exhibit arbitrarily bad singularities, e.g. being in the Sobolev space $H^{1+\beta}$ for arbitrarily small $\beta > 0$, see [12, 13, 23] and references therein.

In this paper we are interested in the elliptic eigenvalue problems which arise in connection with the inverse problems of nondestructive sensing and in the modeling of two phased optic materials (e.g. photonic crystals), see [3–5]. The main feature of these problems is that they are defined by differential operators which have jumping coefficients. Further, these problems depend on a parameter describing material properties. Sometimes varying of the parameter can change dramatically the spectral properties of the eigenvalue problem, e.g. introduce zero eigenvalues.

Computing a zero eigenvalue with floating point arithmetic is always a challenge. The difficulty arises because the important geometric properties, like orthogonality, are only "approximately" realized. Subsequently, numeric pollution might appear. Also, simply shifting away from zero will not solve the problem since shifting strategies do not guarantee high relative numerical accuracy of the computed results.

Date: April 14, 2012.

2000 *Mathematics Subject Classification.* Primary: 65N30, Secondary: 65N25, 65N15.

Key words and phrases. eigenvalue problem, finite element method, a posteriori error estimates .

We tackle this problem using the techniques of relative perturbation theory, for eigenvalues and pseudo inverses, from matrix analysis. In particular we define the penalization based positive definite approximation of the initially given semi definite differential operator (because of Neumann or periodic boundary condition). We study the spectral convergence of the penalization approximation in the limit of the large penalty parameter using the analytic technique from [20]. Assuming a basis for the null space of the operator is explicitly known, we show how to set the penalty parameter which ensures the numerical orthogonality of the computed approximations onto the null space of the operator. This is particularly important for eigenvalue problems (e.g. in photonic crystal applications) where the null space intersects the finite element space only trivially.

The estimation theory from [21] is based on the technique to reduce the study of the approximation properties of a Galerkin eigenvalue approximation to the study of the Galerkin approximation of the solution of the associated source problem, e.g. to the study of the inverse of the associated positive definite differential operator. We generalize this approach, using the theory from [19], to allow us to treat semi-definite eigenvalue problems by reducing them to the study of the generalized inverse of the associated singular operator.

We treat the inverse/pseudo inverse of our operator using the estimation theory for the continuous *hp*-adaptive approximations to the solution of a source problem from [25]. We show efficiency and reliability estimates. In particular, we point out that our reliability constant is independent of the polynomial degree and depends only on the regularity parameter of the *hp*-adaptive approximation.

Finally we report on an extensive numerical study of the proposed estimator. In particular we show that our estimator is robust with respect to the dependence on the parameter of the problem even in the case when for some singular values of the parameter the problem changes type (positive definite problem becomes semi-definite). Also, we show that our estimator is robust with respect to the size of the jump in the coefficients of the differential operator.

We assess the robustness of the estimator by computing the effectivity quotients of the error with the estimator. To approximate the error we either use explicit solutions, when available, or highly accurate numerical solutions. Such highly accurate solutions have been computed by a discontinuous Galerkin method. The accuracy of these benchmark solutions have been assessed by an expensive goal oriented estimator as described in [18].

The paper is organized as follows: In Section 2 we describe the two classes of model problems under consideration, outline the basic theory of such problems, discuss the *hp*-discretization, and introduce the key concept of *approximation defects* and it relation to discretization errors in eigenvalue and invariant subspace computations. Section 3 contains the key results concerning a practical estimation of eigenvalue and invariant subspace discretization errors. Extensive and detailed experiments which demonstrate the performance of our approach are provided in Section 4. Finally, in Section 5 we briefly summarize the key points of this work, and indicate the directions in which we expect further progress to be made.

2. Model problem and approximation defects

We are interested in the eigenvalue problems of the form:

$$\text{Find } (\lambda, \psi) \in \mathbb{R} \times \mathcal{H} \text{ so that } B(\psi, v) = \lambda(\psi, v) \text{ and } \psi \neq 0 \text{ for all } v \in \mathcal{H} \ , \tag{2.1}$$

where $\mathcal{H}$ is a real or complex Hilbert space containing the L^2-integrable functions, B is a positive semi-definite bilinear or sesquilinear form, and (v, w) is the L^2 inner-product on $\mathcal{H}$. We use the standard notation $v \perp w$ to denote that $(v, w) = 0$, $v \perp W$ to denote that $v \perp w$ for all $w \in W$, and $V \perp W$ to denote that $v \perp W$ for all $v \in V$. We consider two classes of problems:

Definition 2.1 (Type I Problems)**.** Let $\Omega \subset \mathbb{R}^2$ be a bounded *polygonal region*, possibly with re-entrant corners. We take $\mathcal{H} := H^1(\Omega)$ as the usual first order Sobolev space over $\mathbb{R}$, and define

$$B(w,v) = \int_\Omega \mathsf{A}\nabla w \cdot \nabla v \,\mathrm{dx}\ , \tag{2.2}$$

where $\mathsf{A} \in [L^\infty(\Omega)]^{2\times 2}$ is uniformly positive definite a.e. As a practical matter, we will further assume that A is piecewise-constant on some polygonal partition of Ω.

Definition 2.2 (Type II Problems)**.** Let $\Gamma = \mathbb{Z}^2$ be a periodicity lattice and let $\mathbb{T}^2 = \mathbb{R}^2/\Gamma$ denote the torus in two dimensions. We define $\mathcal{H} = H^1(\mathbb{T}^2)$ as the usual first order (periodic) Sobolev space over $\mathbb{C}$. For fixed $\kappa \in \mathbb{R}^2$, we define eigenvalue problem defined by the forms

$$B(u,v) = \int_{\mathbb{T}^2} \mathsf{A}(\nabla + \mathrm{i}\kappa)u \cdot \overline{(\nabla + \mathrm{i}\kappa)v}\,\mathrm{dx}\ . \tag{2.3}$$

If we want to emphasize that B corresponds to a Type II problem, we will use κ as a subscript, e.g. B_κ. The matrix $\mathsf{A} \in [L^\infty(\mathbb{T}^2)]^{2\times 2}$ is assumed to be Hermitian positive definite a.e., and again, as a practical matter it is assumed to be piecewise constant on some polygonal partition of $\mathbb{T}^2$.

Here and elsewhere, we use the following standard notation for norms and seminorms: for $k \in \mathbb{N}$ and a domain S we denote the standard norms and semi-norms on the Hilbert spaces $H^k(S)$ by

$$\|v\|_{k,S}^2 = \sum_{|\alpha|\le k} \|D^\alpha v\|_S^2 \qquad\qquad |v|_{k,S}^2 = \sum_{|\alpha|=k} \|D^\alpha v\|_S^2\ , \tag{2.4}$$

where $\|\cdot\|_S$ denotes the L^2 norm on S. When $S = \Omega$ or $S = \mathbb{T}^2$ we omit it from the subscript. We also use the notation

$$|\!|\!| u |\!|\!| = B(u,u)^{1/2} \quad , \quad |\!|\!| u |\!|\!|_\kappa = B_\kappa(u,u)^{1/2}, \kappa \in \mathbb{R}^2,$$

to denote the energy semi-norms of $u \in \mathcal{H}$.

2.1. **Properties of semidefinite model eigenvalue problems.** We define $\mathrm{Ker}(B) := \{u \in \mathcal{H} :\ B(u,u) = 0\}$ and let $N : \mathcal{H} \to \mathrm{Ker}(B)$ be the L^2-orthogonal projection. Noting that $\mathrm{Ker}(B)$ is a closed subspace, we also define $Q = I - N : \mathcal{H} \to \mathrm{Ker}(B)^\perp$ as the L^2-orthogonal projection onto the L^2-orthogonal complement of $\mathrm{Ker}(B)$. Both Q and N are spectral projections for the positive semi-definite self-adjoint operator $\mathcal{A}$ which is defined in the sense of Kato by

$$(\mathcal{A}^{1/2}u, \mathcal{A}^{1/2}v) = B(u,v) \qquad u, v \in \mathcal{H}$$

and $\mathrm{Dom}(\mathcal{A}^{1/2}) = \mathcal{H}$.

For Type I problems, it is clear that $\mathrm{Ker}(B)$ operator consists of the constant functions—these are the eigenfunctions associated with the simple eigenvalue 0. As any reasonable discrete space V will contain the constant functions, this class of problems exemplifies the more general case in which $\mathrm{Ker}(B) \subset V$. For Type II problems it is clear that, for $\kappa \in 2\pi\mathbb{Z}^2$, $\mathrm{Ker}(B)$ is spanned by $\psi_0 = e^{-i\kappa\cdot x}$—this is the unique solution of $(\nabla + i\kappa)\psi = 0$. As before, these are the eigenfunctions associated with the simple eigenvalue 0. The restriction on κ is solely to satisfy the periodicity conditions. When $\kappa = \mathbf{0}$, we are back to the case of constant functions in the kernel, so $\mathrm{Ker}(B) \subset V$. In the more interesting case, $\kappa \in 2\pi\mathbb{Z}^2 \setminus \{\mathbf{0}\}$, for the finite element spaces V described in Subsection 2.2, it is apparent that $\mathrm{Ker}(B) \cap V = \{0\}$. For either type of model problem the dimension of the kernel is (at most) one, but we also consider the more general situation when $\mathrm{Ker}(B)$ has dimension $k \in \mathbb{N}$ in some of our development.

Let $\sigma > 0$ be given, and define $B^\sigma(u,v) = B(u,v) + \sigma(u, Nv)$. For a function $f \in L^2$ we may consider two related source problems:

$$\text{Find } u^+(f) \in \mathcal{H} \text{ such that } B(u^+(f), v) = (Qf, v) \text{ for every } v \in \mathcal{H} \ ,$$
$$\text{Find } u^\sigma(f) \in \mathcal{H} \text{ such that } B^\sigma(u^\sigma(f), v) = (f, v) \text{ for every } v \in \mathcal{H} \ .$$

The choice of notation $u^+(f)$ is due to the fact that, from the algebraic point of view, we are computing the action of the generalized inverse of the operator which is defined by the form B on the vector $f \in L^2$. The latter of these offers an alternative for computing the inverse, via Tikhonov regularization, with "penalty parameter" σ. It holds that

$$\lim_{\sigma \to \infty} u^\sigma(f) = u^+(f) \ ,$$

and we have the estimate

$$0 \le |\!|\!| u^\sigma(f) - u^+(f) |\!|\!|_\sigma^2 = \big(f, u^\sigma(f)\big) - \big(f, u^+(f)\big) \le \frac{C}{\sigma} \ \big(f, f\big) \ ,$$

for the speed of convergence—see [20, Theorem 4.3] and note that N is a spectral projection. The constant C is independent of f, and we use $|\!|\!| v |\!|\!|_\sigma^2 = B^\sigma(v,v)$.

For this paper we assume that the operator $\mathcal{A}$ is such that 0 is an isolated eigenvalue. This means that we can number the nonzero eigenvalues of the operator $\mathcal{A}$ by

$$0 < \lambda_1 \le \lambda_2 \le \cdots \le \lambda_q \le \cdots \ . \tag{2.5}$$

Here we count the nonzero eigenvalues according to their multiplicities. Solutions of the variational eigenvalue problems (2.1) are attained by the positive sequence of eigenvalues (2.5) and a sequence of eigenvectors $(\psi_i)_{i \in \mathbb{N}}$ such that

$$B(\psi_i, v) = \lambda_i (\psi_i, v), \qquad \forall v \in \mathcal{H}, \qquad \text{and } (\psi_i, \psi_j) = \delta_{ij} \ . \tag{2.6}$$

Here and below we count the eigenvalues according to their multiplicity. Furthermore, the sequence $(\lambda_i)_{i \in \mathbb{N}}$ has no finite accumulation point and

$$L^2(\Omega) = \mathrm{Ker}(B) \oplus \mathrm{Cls}(\mathrm{span}\{\psi_j \ : \ j \in \mathbb{N}\}) \ .$$

2.1.1. *Relationship between eigenvalues/vectors of B and B^σ.* In this section we summarize the results of [20] which are relevant for this paper. First note that the form B^σ is positive definite, therefore we use

$$0 < \lambda_1(\sigma) \le \lambda_2(\sigma) \le \cdots \le \lambda_q(\sigma) \le \cdots$$

to denote the eigenvalues of the eigenvalue problem for B^σ, and $(\psi_i(\sigma))_{i \in \mathbb{N}}$ denotes a sequence of eigenvectors which is numbered as in (2.5) and (2.6). Standard monotonicity results (e.g. [27]) imply that

$$\lambda_j(\sigma) \le \lambda_j, \qquad j \in \mathbb{N}$$

and $\lambda_j(\sigma) \to \lambda_j$ as $\sigma \to \infty$, together with multiplicity. Furthermore, a similar result holds for spectral projections.

Let $E(\lambda_q)$ be the L^2 orthogonal projection onto the space $\mathrm{span}\{\psi_j \ : \ j = 1, \cdots, q\}$ and let $E_\sigma(\lambda_q)$ be its orthogonal projection onto $\mathrm{span}\{\psi_i(\sigma) \ : \ \lambda_i(\sigma) \le \lambda_q\}$. We have the following technical result, which follows from [20, Theorem 3.3], [20, Corollary 3.8] and [20, Theorem 4.3]:

Lemma 2.3. *Let* $\mathrm{M} \in \mathbb{N}$ *be given such that* $\lambda_{\mathrm{M}} < \lambda_{\mathrm{M}+1}$. *Then there exists a parameter* σ_0 *and constants* $c_{1,\mathrm{M}}$, $C_{1,\mathrm{M}}$ *and* $C_{2,\mathrm{M}}$ *such that the following estimates hold*

$$\frac{c_{1,\mathrm{M}}}{\sigma} \leq \sum_{i=1}^{\mathrm{M}} \frac{\lambda_j - \lambda_j(\sigma)}{\lambda_j} \leq \frac{C_{1,\mathrm{M}}}{\sigma} \tag{2.7}$$

$$\|E(\lambda_{\mathrm{M}}) - E_\sigma(\lambda_{\mathrm{M}})\|_{HS} \leq \frac{C_{2,\mathrm{M}}}{\sqrt{\sigma}}. \tag{2.8}$$

for all $\sigma > \sigma_0$. *The constants* $C_{1,\mathrm{M}}$ *and* $C_{2,\mathrm{M}}$ *depend solely on the distance between* λ_{M} *and* $\lambda_{\mathrm{M}+1}$ *and the regularity properties of* $\mathrm{Ker}(B)$ *where as the constant* $c_{1,\mathrm{M}}$ *depends on the regularity properties of* $\mathrm{Ker}(B)$ *and the quotient* $\lambda_1/\lambda_{\mathrm{M}}$. *The norm* $\|\cdot\|_{HS}$ *is the Hilbert-Schmidt norm on the space of compact operators (Hilbert-Schmidt operators are those compact operators* A *such that operator* A^*A *has a finite trace and then* $\|A\|_{HS} = \sqrt{tr(A^*A)}$*).*

2.2. **Discrete eigenvalue/eigenvector approximations.** We discretize (2.1) using *hp*-finite element spaces, which we now briefly describe. Let $\mathcal{T} = \mathcal{T}_h$ be a triangulation of Ω with the piecewise-constant mesh function $h : \mathcal{T}_h \to (0,1)$, $h(K) = \mathrm{diam}(K)$ for $K \in \mathcal{T}_h$. Throughout we implicitly assume that the mesh is aligned with all discontinuities of the data A. Given a piecewise-constant distribution of polynomial degrees, $p : \mathcal{T}_h \to \mathbb{N}$, we define the space

$$V = V_h^p = \{v \in \mathcal{H} \cap C(\overline{\Omega}) : \ v\big|_K \in \mathbb{P}_{p(K)} \text{ for each } K \in \mathcal{T}_h\} \ ,$$

where $\mathbb{P}_j$ is the collection of polynomials of total degree no greater than j on a given set. Suppressing the mesh parameter h for convenience, we also define the set of edges $\mathcal{E}$ in $\mathcal{T}$, and distinguish interior edges $\mathcal{E}_I$, and edges on the boundary $\mathcal{E}_N$. Additionally, we let $\mathcal{T}(e)$ denote the one or two triangles having $e \in \mathcal{E}$ as an edge, and we extend p to $\mathcal{E}$ by $p(e) = \max_{K \in \mathcal{T}(e)} p(K)$. As is standard, we assume that the family of spaces satisfy the following regularity properties on $\mathcal{T}_h$ and p: There is a constant $\gamma > 0$ for which

(C1) $\gamma^{-1}[h(K)]^2 \leq \mathrm{area}(K)$ for $K \in \mathcal{T}$,
(C2) $\gamma^{-1}(p(K)+1) \leq p(K')+1 \leq \gamma(p(K)+1)$ for adjacent $K, K' \in \mathcal{T}$, $\overline{K} \cap \overline{K'} \neq \emptyset$.

It is really just a matter of notational convenience that a single constant γ is used for all of these upper and lower bounds. The shape regularity assumption (C1) implies that the diameters of adjacent elements are comparable.

In what follows we consider the discrete versions of (2.1):

$$\text{Find } (\hat{\lambda}, \hat{\psi}) \in \mathbb{R} \times V \text{ such that } B(\hat{\psi}, v) = \hat{\lambda}(\hat{\psi}, v) \text{ for all } v \in V \ . \tag{2.9}$$

We also assume, without further comment, that the solutions are ordered and indexed as in (2.5), with $(\hat{\psi}_i, \hat{\psi}_j) = \delta_{ij}$. That is to say we have

$$0 < \hat{\lambda}_1 \leq \hat{\lambda}_2 \leq \cdots \leq \hat{\lambda}_{N_Z}.$$

More to the point, we assume that either $\mathrm{Ker}(B) \cap V = \{0\}$ or $\mathrm{Ker}(B) \subset V$ and obviously $N_Z \leq \dim V$.

We are interested in assessing approximation errors in collections of computed eigenvalues and associated invariant subspaces. Let $s_m = \{\mu_k\}_{k=1}^m \subset (a,b)$ be the set of all eigenvalues of B, counting multiplicities, in the interval (a,b), $a > 0$, and let $S_m = \mathrm{span}\{\phi_k\}_{k=1}^m$ be the associated invariant subspace, with $(\phi_i, \phi_j) = \delta_{ij}$. The discrete problem (2.9) is used to compute corresponding approximations $\hat{s}_m = \{\hat{\mu}_k\}_{k=1}^m$ and $\hat{S}_m = \mathrm{span}\{\hat{\phi}_k\}_{k=1}^m$, with $(\hat{\phi}_i, \hat{\phi}_j) = \delta_{ij}$.

Remark 2.4. When s_m consists of the smallest m positive eigenvalues, we use the absolute labeling $s_m = \{\lambda_k\}_{k=1}^m$ and $S_m = \mathrm{span}\{\psi_k\}_{k=1}^m$ instead of the relative labeling involving (μ_k, ϕ_k); and the analogous statement holds for the discrete approximations $\hat{s}_m$ and $\hat{S}_m$.

2.3. **Approximation defects.** Let the finite element space $V \subset \mathcal{H}$ be given and let $\hat{s}_m$ and $\hat{S}_m$ be the approximations which are computed from V. We define the *approximation defects* in $\hat{s}_m, \hat{S}_m$ as:

$$\eta_i^2(\hat{S}_m) = \max_{\substack{\mathcal{S}\subset\hat{S}_m \\ \dim\mathcal{S}=m-i+1}} \min_{\substack{f\in\mathcal{S} \\ f\neq 0}} \frac{\|\!|u^+(f)-\hat{u}^+(f)|\!\|^2}{\|\!|u^+(f)|\!\|^2}\ , \tag{2.10}$$

where $u^+(f)$ and $\hat{u}(f)$ satisfy:

$$B(u^+(f),v) = (Qf,v) \text{ for every } v\in\mathcal{H} \tag{2.11}$$

$$B(\hat{u}^+(f),v) = (Qf,v) \text{ for every } v\in V\ . \tag{2.12}$$

We will argue below that such approximation defects are very useful for estimating the error in $\hat{s}_m$ as an approximation of s_m (and $\hat{S}_m$ as an approximation of S_m).

Of course, $u^+(f)$, and hence η_i, cannot be computed, so we must efficiently and reliably estimate these quantities. For positive definite forms, we have shown in [21] how to use hierarchical basis error estimators (cf. [9]) to efficiently and reliably estimate η_i in the case of low-order h-elements; and in [17] how to similarly use residual-based error estimators (cf. [14]) in the case of hp-elements. The present work extends the latter approach to the case of semi-definite forms, and we elaborate on the details in Section 3.

We will state the following geometrical lemma, which follows from [19], and indicates what type of information is encoded in the approximation defects.

Lemma 2.5. *Let* $\mathcal{C}_m = \{\psi\in\mathrm{Ker}(B)\ :\ \psi\perp\hat{S}_m\}$ *and let* $\eta_m(\hat{S}_m)<1$. *Then*

$$\mathrm{Ker}(B) = (\mathrm{Ker}(B)\cap\hat{S}_m)\oplus\mathcal{C}_m.$$

The approximation defects are related to the eigenvalue error in the following way. Assume that $\hat{S}_{\mathrm{M}}$ is the span of first $\mathrm{M}\in\mathbb{N}$ eigenvectors of (2.5) then we have the following efficiency and reliability result.

Theorem 2.6. *Let* $B(\cdot,\cdot)$ *be the any of the semi-definite forms given in (2.2) and (2.3) and let* $\lambda_{\mathrm{M}}<\lambda_{\mathrm{M}+1}$. *If* $\hat{S}_{\mathrm{M}}=\mathrm{span}\{\hat{\psi}_1,\cdots,\hat{\psi}_{\mathrm{M}}\}$ *is such that* $\frac{\eta_{\mathrm{M}}(\hat{S}_{\mathrm{M}})}{1-\eta_{\mathrm{M}}(\hat{S}_{\mathrm{M}})} < \frac{\lambda_{\mathrm{M}+1}-\hat{\lambda}_{\mathrm{M}}}{\lambda_{\mathrm{M}+1}+\hat{\lambda}_{\mathrm{M}}}$ *then*

$$\frac{\hat{\lambda}_1}{2\hat{\lambda}_{\mathrm{M}}}\sum_{i=1}^{\mathrm{M}}\eta_i^2(\hat{S}_{\mathrm{M}}) \le \sum_{i=1}^{\mathrm{M}}\frac{\hat{\lambda}_i-\lambda_i}{\hat{\lambda}_i} \le C_{\mathrm{M}}\sum_{i=1}^{\mathrm{M}}\eta_i^2(\hat{S}_{\mathrm{M}}). \tag{2.13}$$

The constant C_M, *depends solely on the relative distance to the unwanted component of the spectrum (e.g.* $\frac{\lambda_{\mathrm{M}}-\lambda_{\mathrm{M}+1}}{\lambda_{\mathrm{M}}+\lambda_{\mathrm{M}+1}}$*).*

Proof. The fact that $0<\hat{\lambda}_i$, $i=1,\cdots\mathrm{M}$ and Lemma 2.5 imply the conclusion $\hat{S}_{\mathrm{M}}\perp\mathrm{Ker}(B)$. The problem can now be reduced to the study of the positive definite form

$$B^\infty(u,v)=B(u,v),\qquad u,v\in\mathrm{Dom}(B^\infty)=\{\psi\in\mathcal{H}\ :\ \psi\perp\mathrm{Ker}(B)\}.$$

Furthermore, we have that

$$\eta_i^2(\hat{S}_m)=\eta_{i,\infty}^2(\hat{S}_m)$$

where $\eta_{i,\infty}^2(\hat{S}_m)$ denotes the approximation defects for the form B^∞ and the subspace $\hat{S}_m\subset\mathrm{Dom}(B^\infty)$ as defined in [21]. The statement of the theorem follows by [8, Theorem 3.10]. Q.E.D.

The constant C_{M} is given by an explicit formula which is a reasonable practical overestimate, see [8, 21] for details. A similar results holds for the eigenvectors. We point the interested reader to [21, Theorem 4.1 and equation (3.10)] and [8, Theorem 3.10].

Remark 2.7. If $\lambda_1=\lambda_{\mathrm{M}}$, then the constant $\hat{\lambda}_1/2\hat{\lambda}_{\mathrm{M}}$ in (2.13) can be replaced by 1.

3. Practical error estimators for the *hp*-adaptive method

3.1. **The Case** $\mathrm{Ker}(B) \subset V$**.** This case covers all Type I problems, as well as Type II problems when $\kappa = \mathbf{0}$. When $\mathrm{Ker}(B) \subset V$, we work directly with the approximation defects from (2.10). We have the following modification of [17, Lemma 3.4].

Lemma 3.1. *It holds that*

$$\frac{1}{1+\mathfrak{D}_l}\sum_{i=1}^{m}\hat{\mu}_i^{-1}|\!|\!|u^+(\hat{\mu}_i\hat{\phi}_i)-\hat{u}^+(\hat{\mu}_i\hat{\phi}_i)|\!|\!|^2 \le \sum_{i=1}^{m}\eta_i^2(\hat{S}_m) \le \sum_{i=1}^{m}\hat{\mu}_i^{-1}|\!|\!|u^+(\hat{\mu}_i\hat{\phi}_i)-\hat{u}^+(\hat{\mu}_i\hat{\phi}_i)|\!|\!|^2 \ . \tag{3.1}$$

The constant $\mathfrak{D}_l$ *was defined in* [17].

We must estimate $|\!|\!|u^+(\hat{\mu}_i\hat{\phi}_i)-\hat{u}^+(\hat{\mu}_i\hat{\phi}_i)|\!|\!|^2$ for each Ritz vector, where $\hat{S}_m = \mathrm{span}\{\hat{\phi}_1,\ldots,\hat{\phi}_m\}$ is our approximation of $S_m = \mathrm{span}\{\phi_1,\ldots,\phi_m\}$. We modify key results from [17], which were stated only for in the positive definite case to our context. The identity $\hat{u}^+(\hat{\mu}_i\hat{\phi}_i) = \hat{\phi}_i$, makes our job easier. We define the element residuals R_i for $K \in \mathcal{T}$, and the edge (jump) residuals r_i for $e \in \mathcal{E}$, by

$$R_i|_K = \hat{\mu}_i\hat{\phi}_i + \nabla\cdot A\nabla\hat{\phi}_i \quad , \quad r_i|_e = \begin{cases} -(A\nabla\hat{\phi}_i)_{|_K}\cdot\mathbf{n}_K - (A\nabla\hat{\phi}_i)_{|_{K'}}\cdot\mathbf{n}_{K'} & , e\in\mathcal{E}_I \\ -(A\nabla\hat{\phi}_i)_{|_K}\cdot\mathbf{n}_K & , e\in\mathcal{E}_N \end{cases} , \tag{3.2}$$

for Type I problems and Type II problems with $\kappa = \mathbf{0}$. For interior edges $e \in \mathcal{E}_I$, K and K' are the two adjacent elements, having outward unit normals $\mathbf{n}_K$ and $\mathbf{n}_{K'}$, respectively; and for boundary edges $e \in \mathcal{E}_N$, K is the single adjacent element, having outward unit normal $\mathbf{n}_K$. We note that R is a polynomial of degree no greater than $p(K)$ on K, and r is a polynomial of degree no greater than $p(e)-1$ on e.

Our estimate of $\varepsilon_i^2 = \sum_{K\in\mathcal{T}}\varepsilon_i^2(K) \approx |\!|\!|u^+(\hat{\mu}_i\hat{\phi}_i)-\hat{u}^+(\hat{\mu}_i\hat{\phi}_i)|\!|\!|^2$ is computed from local quantities,

$$\varepsilon_i^2(K) = \left(\frac{h(K)}{p(K)}\right)^2\|R_i\|_{0,K}^2 + \frac{1}{2}\sum_{e\in\mathcal{E}_I(K)}\frac{h(e)}{p(e)}\|r_i\|_{0,e}^2 + \sum_{e\in\mathcal{E}_N(K)}\frac{h(e)}{p(e)}\|r_i\|_{0,e}^2 \ , \tag{3.3}$$

where $\mathcal{E}_I(K)$ and $\mathcal{E}_N(K)$ denote the interior edges and boundary edges of K, respectively.

The following analogues of [17, Lemma 4.1, Lemma 4.2] carry over directly in this case.

Lemma 3.2. *The following holds for Type I and Type II problems for which* $\mathrm{Ker}(B) \subset V$*. There is a constant* $C > 0$*, depending only on the hp-constant* γ *and* $\lambda_{\min}(\mathsf{A})$*, such that* $|\!|\!|u^+(\hat{\mu}_i\hat{\phi}_i) - \hat{u}^+(\hat{\mu}_i\hat{\phi}_i)|\!|\!|^2 \le C\varepsilon_i^2$*. Furthermore, for any* $\epsilon > 0$*, there is a constant* $c = c(\epsilon) > 0$*, depending only on the hp-constant* γ *and* $\|B\|$*, such that* $\varepsilon_i^2(K) \le cp_K^{2+2\epsilon}|\!|\!|u^+(\hat{\mu}_i\hat{\phi}_i) - \hat{u}^+(\hat{\mu}_i\hat{\phi}_i)|\!|\!|_{\omega_K}^2$.

With this we have

Theorem 3.3. *Under the assumptions of Theorem 2.6, we have the following upper- and lower-bounds on eigenvalue error,*

$$C_1\sum_{i=1}^{\mathrm{M}}\hat{\lambda}_i^{-1}\varepsilon_i^2 \le \sum_{i=1}^{\mathrm{M}}\frac{\hat{\lambda}_i-\lambda_i}{\hat{\lambda}_i} \le C_2\sum_{i=1}^{\mathrm{M}}\hat{\lambda}_i^{-1}\varepsilon_i^2 \ . \tag{3.4}$$

The constant C_1 *depends solely on the ratio* $\hat{\lambda}_1/(2\hat{\lambda}_2)$*, the hp-regularity constant* γ*, the continuity constant* $\|B\|$*, and the maximal polynomial degree* $\bar{p} = \max_{K\in\mathcal{T}}p(K)$*. The constant* C_2 *depends solely on the relative distance to the unwanted component of the spectrum, the hp-regularity constant* γ *and* $\lambda_{\min}(\mathsf{A})$*.*

3.2. **The Case** $\mathrm{Ker}(B) \cap V = \{0\}$**.** Although the Type II problems of this sort have a one-dimensional kernel, we consider the more general situation of a k-dimensional kernel. Here we employ the penalized form B^σ, which yields a positive definite eigenvalue problem. The σ-dependence of the corresponding discrete eigenpairs $(\hat\lambda_i\,,\,\hat\psi_i) = (\hat\lambda_i(\sigma)\,,\,\hat\psi_i(\sigma))$ or $(\hat\mu_i\,,\,\hat\phi_i) = (\hat\mu_i(\sigma)\,,\,\hat\phi_i(\sigma))$ should be understood even when it is suppressed for notational convenience. Also, we use the notation $\hat E(\lambda_{\mathrm{M}})$ to denote the orthogonal projection onto the space $\mathrm{span}\{\hat\psi_i(\sigma)\ :\ \hat\lambda_i(\sigma) \le \lambda_{\mathrm{M}}\}$

We let $\{z_1, \ldots, z_k\}$ be an orthonormal basis of eigenfunctions for $\mathrm{Ker}(B)$, so

$$B^\sigma(u,v) = B(u,v) + \sigma(u, Nv) = B(u,v) + \sigma \sum_{j=1}^{k} (u, z_j)\,(z_j, v) \tag{3.5}$$

If $\{v_1, \ldots, v_N\}$ is a standard (locally supported) basis for V, it is clear from (3.5) that the stiffness associated with B^σ and this basis will be the sum of a sparse matrix and one which is of (at most) rank k. In this sense the stiffness matrix is "data-sparse", because its action on a vector is an $\mathcal{O}(N)$ computation.

Using a Cauchy inequality (with δ), we see that

$$|\!|\!| v |\!|\!|_\sigma^2 \ge (1-\delta)\,\lambda_{\min}(\mathsf{A})\,|v|_{1,\mathbb{T}^2}^2 - \left(\frac{1}{\delta} - 1\right) \lambda_{\max}(\mathsf{A})\,\|\kappa\|_{\ell_2}^2\,\|v\|_{0,\mathbb{T}^2}^2 + \sigma \|Nv\|_{0,\mathbb{T}^2}^2\ ,$$

for any $\delta > 0$. So although B^σ is not coercive with respect to $|\cdot|_{1,\mathbb{T}}$, in the sense that we cannot guarantee that $|\!|\!| v |\!|\!|_\sigma \ge m_0 |v|_{1,\mathbb{T}}$ for some m_0 which is independent of $v \in \mathcal{H}$, a Gårding does hold,

$$|\!|\!| v |\!|\!|_\sigma^2 + \rho \|v\|_{0,\mathbb{T}^2}^2 \ge m_0^2 |v|_{1,\mathbb{T}^2}^2\ ,$$

with $\rho = (1/\delta - 1)\lambda_{\max}(\mathsf{A})\,\|\kappa\|_{\ell_2}^2$ and $m_0^2 = (1-\delta)\lambda_{\min}(\mathsf{A})$, for example. In our derivation of error estimates for Type II with $\kappa \neq \mathbf{0}$, we consider the (further) modified form

$$B^{\sigma,\rho}(u,v) = B^\sigma(u,v) + \rho(u,v)\ ,$$

with corresponding norm $|\!|\!| v |\!|\!|_{\sigma,\rho} \ge m_0 |v|_{1,\mathbb{T}}$. It is clear that $(\lambda, \psi) = (\lambda(\sigma), \psi(\sigma))$ is an eigenpair for B^σ if and only if $(\lambda + \rho, \psi)$ is an eigenpair for $B^{\sigma,\rho}$, and that the analogous assertion holds on the discrete level as well. This spectrum-shifting trick has been used elsewhere (cf. [16]) for similar theoretical arguments, and we will see below that it has no effect on practical implementation.

We motivate our choice of error estimates as follows: Suppose that $(\hat\lambda, \hat\psi) \in \mathbb{R}^+ \times V$ satisfies $B^\sigma(\hat\psi, v) = \hat\lambda\,(\hat\psi, v)$ for all $v \in V$. As stated above, $B^{\sigma,\rho}(\hat\psi, v) = (\hat\lambda + \rho)\,(\hat\psi, v)$ for all $v \in V$. We set $f = (\hat\lambda + \rho)\hat\psi$ and define $u(f) \in \mathcal{H}$ and $\hat u(f) \in V$ by

$$B^{\sigma,\rho}(u(f), v) = (f, v) \text{ for all } v \in \mathcal{H} \quad , \quad B^{\sigma,\rho}(\hat u(f), v) = (f, v) \text{ for all } v \in V\ .$$

It is clear that $\hat u(f) = \hat\psi$. We now go through the usual steps for deriving residual-based error estimates for boundary value problems. For any $v \in \mathcal{H}$ and $\hat v \in V$,

$$\begin{aligned} B^{\sigma,\rho}(u(f) - \hat u(f), v) &= B^{\sigma,\rho}(u(f) - \hat u(f), v - \hat v) = (f, v - \hat v) - B^{\sigma,\rho}(\hat u(f), v - \hat v) \\ &= \left(\hat\lambda\hat\psi - \sigma \sum_{j=1}^{k} (\hat\psi, z_j) z_j\ , v - \hat v \right) - B(\hat\psi, v - \hat v) \\ B(\hat\psi, v - \hat v) &= \sum_{K \in \mathcal{T}} \left(\int_{\partial K} \mathsf{A}(\nabla + i\kappa)\hat\psi \cdot \mathbf{n}\,(v - \hat v)\,ds - \int_K (\nabla + i\kappa) \cdot \mathsf{A}(\nabla + i\kappa)\hat\psi\,(v - \hat v)\,dx \right) \end{aligned}$$

We emphasize that the quantity on the right-hand side is independent of ρ. Choosing the element and edge residuals

$$R^\sigma|_K = \left(\hat{\lambda}\hat{\psi} + (\nabla + i\kappa)\cdot \mathsf{A}(\nabla + i\kappa)\hat{\psi} - \sigma \sum_{j=1}^{k} (\hat{\psi}, z_j)\, z_j \right)_{|_K} \tag{3.6}$$

$$r^\sigma|_e = \begin{cases} -(\mathsf{A}(\nabla + i\kappa)\hat{\psi})_{|_K} \cdot \mathbf{n}_K - (\mathsf{A}(\nabla + i\kappa)\hat{\psi})_{|_{K'}} \cdot \mathbf{n}_{K'} & , e \in \mathcal{E}_I \\ -(\mathsf{A}(\nabla + i\kappa)\hat{\psi})_{|_K} \cdot \mathbf{n}_K & , e \in \mathcal{E}_N \end{cases} , \tag{3.7}$$

we naturally define the error estimate $\varepsilon_\sigma^2 \approx |\!|\!| u(f) - \hat{u}(f) |\!|\!|_{\sigma,\rho}^2$ by

$$\varepsilon_\sigma^2 = \sum_{K \in \mathcal{T}} \varepsilon_\sigma^2(K) \tag{3.8}$$

$$\varepsilon_\sigma^2(K) = \left(\frac{h(K)}{p(K)} \right)^2 \|R^\sigma\|_{0,K}^2 + \frac{1}{2} \sum_{e \in \mathcal{E}_I(K)} \frac{h(e)}{p(e)} \|r^\sigma\|_{0,e}^2 + \sum_{e \in \mathcal{E}_N(K)} \frac{h(e)}{p(e)} \|r^\sigma\|_{0,e}^2 \ . \tag{3.9}$$

At this stage, Cauchy-Schwarz inequalities (both continuous and discrete) and interpolation error estimates yield

$$|\!|\!| u(f) - \hat{u}(f) |\!|\!|_{\sigma,\rho}^2 \le C \varepsilon_\sigma |u(f) - \hat{u}(f)|_{1,\mathbb{T}} \le \frac{C}{m_0}\, \varepsilon_\sigma\, |\!|\!| u(f) - \hat{u}(f) |\!|\!|_{\sigma,\rho} \ ,$$

for some C which depends only on the mesh parameter γ. From this we deduce, via the obvious bound $|\!|\!| u(f) - \hat{u}(f) |\!|\!|_\sigma \le |\!|\!| u(f) - \hat{u}(f) |\!|\!|_{\sigma,\rho}$, that

Lemma 3.4. *If $(\hat{\lambda}, \hat{\psi}) \in \mathbb{R}^+ \times V$ is a discrete eigenpair for B^σ, and we choose $f = (\hat{\lambda} + \rho)\hat{\psi}$ for ρ sufficiently large (see above discussion), then*

$$|\!|\!| u(f) - \hat{u}(f) |\!|\!|_\sigma \le \frac{C}{m_0}\, \varepsilon_\sigma \ ,$$

where C depends only on the mesh parameter γ, and m_0 depends only on $\lambda_{\min}(\mathsf{A})$.

The (strong) residuals R^σ and r^σ are naturally functions on $\mathbb{R}^+ \times V$, with $R^\sigma = R^\sigma(\hat{\lambda}, \hat{\psi})$ and $r^\sigma = r^\sigma(\hat{\lambda}, \hat{\psi})$ given in (3.6)-(3.7). For a collection of discrete eigenpairs $s_m = \{(\hat{\mu}_i, \hat{\phi}_i) : 1 \le i \le m\}$ for B^σ we define the corresponding residuals $R^{\sigma,i} = R^\sigma(\hat{\mu}_i, \hat{\phi}_i)$ and $r^{\sigma,i} = r^\sigma(\hat{\mu}_i, \hat{\phi}_i)$, and define $\varepsilon_{i,\sigma}$ from $R^{\sigma,i}$ and $r^{\sigma,i}$ as in (3.8)-(3.9). We remark that, although we have stated these definitions in the relative numbering (a collection anywhere in the spectrum), Theorem 3.5 concerns the first M positive eigenvalues, and therefore uses the absolute numbering $(\hat{\lambda}_i, \hat{\psi}_i)$. We now state the main theorem in this context as a combination of Lemma 2.3 and [17, Theorem 4.4].

Theorem 3.5. *Let $\mathrm{Ker}(B) \cap V = \{0\}$ and let $\mathrm{M} \in \mathbb{N}$ be such that $\lambda_{\mathrm{M}} < \lambda_{\mathrm{M}+1}$. Then for $\sigma > \sigma_0$*

$$\sum_{i=1}^{\mathrm{M}} \frac{|\hat{\lambda}_i(\sigma) - \lambda_i|}{\lambda_i} \le C_2 \sum_{i=1}^{\mathrm{M}} \hat{\lambda}_i^{-1}(\sigma) \varepsilon_{i,\sigma}^2 + \frac{C_{1,\mathrm{M}}}{\sigma} \tag{3.10}$$

$$\|E(\lambda_{\mathrm{M}}) - \hat{E}_\sigma(\lambda_{\mathrm{M}})\|_{HS} \le C_3 \sqrt{\sum_{i=1}^{\mathrm{M}} \hat{\lambda}_i^{-1}(\sigma) \varepsilon_{i,\sigma}^2} + \frac{C_{2,\mathrm{M}}}{\sqrt{\sigma}}. \tag{3.11}$$

The constants $C_{1,\mathrm{M}}$ and $C_{2,\mathrm{M}}$ are precisely as in Lemma 2.3, and the constants C_2 and C_3 depend solely on the hp-constant γ, $\lambda_{\min}(\mathsf{A})$ and the distance to the unwanted component of the spectrum.

Proof. The proof of (3.10) is an obvious combination, by the use of the triangle inequality, of Lemma 2.3, Lemma 3.4 and [17, Theorem 4.4]. We will concentrate on proving (3.11). Let σ_0 be as given by Lemma 2.3. Recall that the form $B^\sigma(\cdot,\cdot)$ is positive definite. Then using [20, Theorem 3.3] we establish that there exists a constant C_S which depends solely on the distance between $\lambda_{\mathrm{M}+1}(\sigma)$ and $\hat{\lambda}_{\mathrm{M}}(\sigma)$ such that

$$\|E_\sigma(\lambda_{\mathrm{M}}) - \hat{E}_\sigma(\lambda_{\mathrm{M}})\|_{HS} \leq C_S \sqrt{\sum_{i=1}^{\mathrm{M}} \eta_i^2(\sigma)}.$$

Here $\eta_i^2(\sigma)$ is defined by the formula

$$\eta_i^2(\sigma) = \max_{\substack{\mathcal{S}\subset\hat{S}_{\mathrm{M}} \\ \dim\mathcal{S}=m-i+1}} \min_{\substack{f\in\mathcal{S} \\ f\neq 0}} \frac{|||u(f)-\hat{u}(f)|||_\sigma^2}{|||u(f)|||_\sigma^2}, \qquad i=1,\cdots,\mathrm{M},$$

and $\hat{S}_{\mathrm{M}} = \mathrm{span}\{\hat{\psi}_i(\sigma) \ : \ \hat{\lambda}_i(\sigma) \leq \lambda_{\mathrm{M}}\}$. Assume that the space V_h^p is such that the assumptions of Theorem 2.6 hold for the form B^σ, that is let

$$\frac{\eta_{\mathrm{M}}(\sigma)}{1-\eta_{\mathrm{M}}(\sigma)} < \frac{\lambda_{\mathrm{M}+1}(\sigma) - \hat{\lambda}_{\mathrm{M}}(\sigma)}{\lambda_{\mathrm{M}+1}(\sigma) + \hat{\lambda}_{\mathrm{M}}(\sigma)}$$

then $\dim \hat{S}_{\mathrm{M}} = \mathrm{M}$. The conclusion of the theorem now follows from the triangle inequality for the Hilbert-Schmidt norm and Lemmas 2.3 and 3.4. Q.E.D.

Theorem 3.5 implies that it would be reasonable to set $\sigma = (\dim V\mathbf{u})^{-2}$ as our penalty parameter, where $\mathbf{u} \approx 10^{-16}$ is the unit roundoff. Recall that the scalar product in the finite element space V can be computed up to the accuracy of $O(\dim V\mathbf{u})$ and that $\|E(\lambda_{\mathrm{M}}) - E_\sigma(\lambda_{\mathrm{M}})\|_{HS}$ is a measure of the sine of the largest angle which a vector from $\mathrm{Ran}(E(\lambda_{\mathrm{M}})) = \mathrm{span}\{\psi_i \ : \ \lambda_i \leq \lambda_{\mathrm{M}}\}$ can have with a vector from $\mathrm{Ran}(E_\sigma(\lambda_{\mathrm{M}})) = \mathrm{span}\{\psi_i(\sigma) \ : \ \lambda_i(\sigma) \leq \lambda_{\mathrm{M}}\}$. Setting $\sigma = (\dim V\mathbf{u})^{-2}$ implies that the angle between eigenvectors $\psi_i(\sigma)$, $i=1,\cdots,\mathrm{M}$ of the auxiliary problem and the target eigenvectors ψ_i, $i=1,\cdots,\mathrm{M}$ is on the order of the accuracy with which a sine of an angle can be evaluated. Subsequently, for an arithmetic with such a rounding constant $\mathbf{u}$ vectors $\hat{\psi}_i(\sigma)$, $i=1,\cdots,\mathrm{M}$ are as good approximations of ψ_i, $i=1,\cdots,\mathrm{M}$ as they are of $\psi_i(\sigma)$, $i=1,\cdots,\mathrm{M}$.

4. Experiments

In this section we have collected numerical results regarding our a posteriori error estimator with the clear aim to show the efficiency of the error estimator and the exponential converge of the error on a sequence of *hp*-adapted meshes. Following [7], we assume an error model of the form

$$\hat{\lambda}_i = \lambda_i + Ce^{-2\alpha\sqrt{\mathrm{DOFs}}}$$

for problems whose eigenfunctions are expected to be smooth, and

$$\hat{\lambda}_i = \lambda_i + Ce^{-2\alpha\sqrt[3]{\mathrm{DOFs}}},$$

for problems such as those on non-convex polygonal domains and/or discontinuous coefficients, whose eigenfunctions are expected to have isolated singularities. The constants C and α are determined by least-squares fitting, and α is reported for each problem. Plots are given of the total relative error, its *a posteriori* estimate, and the associated effectivity index, shown, respectively, below:

$$\sum_{i=1}^{\mathrm{M}} \frac{\hat{\lambda}_i - \lambda_i}{\hat{\lambda}_i} \quad , \quad \sum_{i=1}^{\mathrm{M}} \hat{\lambda}_i^{-1}\varepsilon_i^2 \quad , \quad \frac{\sum_{i=1}^{\mathrm{M}} \frac{\hat{\lambda}_i-\lambda_i}{\hat{\lambda}_i}}{\sum_{i=1}^{\mathrm{M}} \hat{\lambda}_i^{-1}\varepsilon_i^2} \ .$$

In the case of a single eigenvalue λ_i the effectivity index reduces $(\hat{\lambda}_i - \lambda_i)/\varepsilon_i^2$, and we make the following comparison with what is presented in [6], in which *hp*-adaptivity is also used for eigenvalue problems. The effectivities reported in [6] are in terms of eigen*function* error, which corresponds closely with the square root of the effectivities reported here. This difference should be taken into consideration when comparing the effectivities reported here with those in [6] or other similar contributions. For problems in which the exact eigenvalues are known, we use these values in our error analysis. For most problems, we use highly accurate computations on very large problems to produce "exact eigenvalues" for our comparisons, as discussed in the introduction.

All the experiments have been carried out using the AptoFEM package (`www.aptofem.com`) on a single processor desktop machine. In particular, we used ARPACK [1] to compute the eigenvalues and MUMPS [2] to solve the linear systems. The adaptive algorithm that we use is very simple: initially we choose the indexes j of the eigenvalues that we want to follow, then starting from a coarse mesh with polynomial degree equal to two we compute the eigenpairs $(\lambda_{j,hp}, \psi_{j,hp})$ and the error estimator. After this we mark elements for refinement using a simple fixed-fraction strategy based on values the values of the error estimator for each element, with 25% refinement, 5% de-refinement; the choice between refining the marked elements in h or p is made by using the technique in [22] to estimate the local analyticity of the exact eigenfunction. Finally, a refined mesh is generated and the process restarted from the computation of the eigenpairs $(\lambda_{j,hp}, \psi_{j,hp})$ on this refined mesh. Included in the convergence plots are comparisons with an h-adaptive method with quadratic elements, which is based on the same error estimation approach.

4.1. **Unit Triangle.** As a simple problem for which the eigenvalues and eigenfunctions are explicitly known (cf. [24]), we consider the Type I problem with $\mathsf{A} = I$ and Ω is the equilateral triangle of having unit edge-length. The eigenvalues can be indexed as

$$\lambda_{mn} = \frac{16\pi^2}{9}(m^2 + mn + n^2)$$

for $0 \leq m \leq n$, and we refer interested readers to [24] for explicit descriptions of the eigenfunctions.

In Figure 1 we plot the total relative errors for the first two eigenvalues, together with the associated error estimates using either h-adaptivity or *hp*-adaptivity. In this case we have obtained $\alpha = 0.3748$. In Figure 2 we plot the effectivity quotient for the $hp-$adaptivity. It is clear that the convergence of the *hp*-adaptive method is exponential and faster than with h-adaptivity alone. Moreover the error estimator seems to be robust.

4.2. **Triangle with Triangular Hole.** Here we again consider a Type I problem with $\mathsf{A} = I$, where Ω is the equilateral triangle having edge-length 2 with an equilateral triangle having edge-length 1/2 removed from its center (see Figure 3).

We now consider the same problem as in the previous example, but in this case, the exact eigenvalues are unknown, so we computed the following reference value for the first eigenvalue, which has multiplicity two, on a very large problem: 3.5591592. This value is accurate at least up to 1e-6.

In Figure 4 we plot the relative errors and error estimates for the first two eigenvalues for both the h-adaptive method and *hp*-adaptive method. In this case we have obtained $\alpha = 0.2539$. In Figure 5 we plot the corresponding values of the effectivity quotient for the *hp*-adaptive method. We again see exponential convergence for the *hp*-adaptive method and clearly only polynomial convergence for the h-adaptive method, which is consistent with the theory.

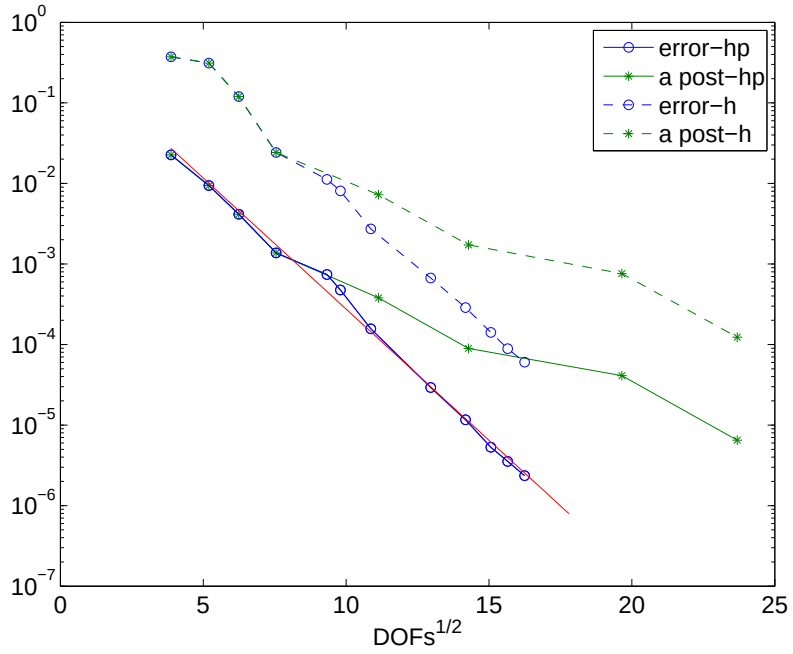

FIGURE 1. Errors and error estimates. Triangle problem.

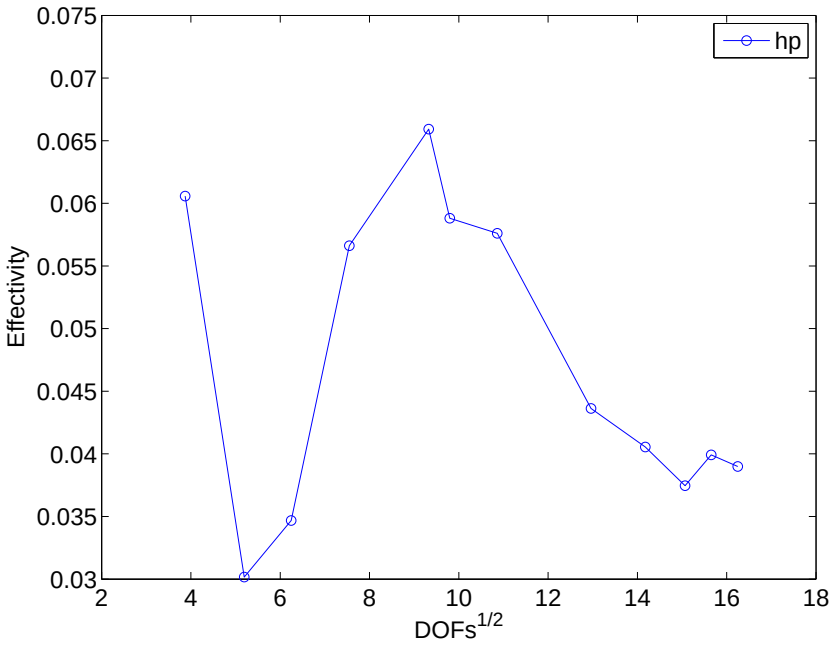

FIGURE 2. Effectivity index. Triangle problem.

4.3. **Unit Square.** Another standard problem with known eigenvalues is the Neumann Laplacian on the unit square (Type I, with $\mathsf{A} = I$), for which we have

$$\lambda_{mn} = (m^2 + n^2)\pi^2 \quad , \quad \psi_{mn} = \cos(m\pi x)\,\cos(n\pi x) \quad , \quad m, n \geq 0 \ .$$

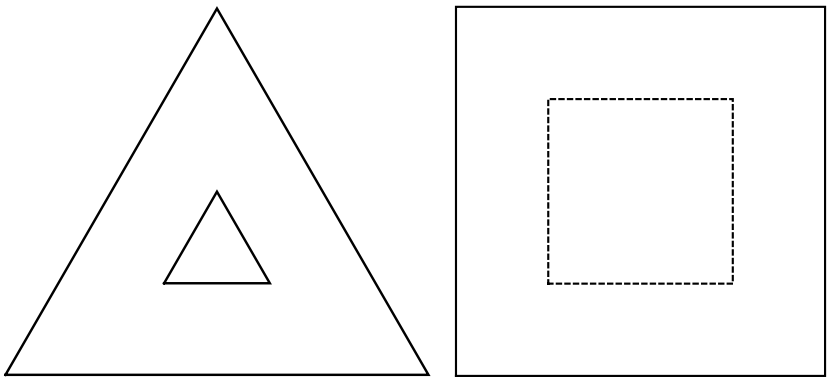

FIGURE 3. Some domains used in experiments.

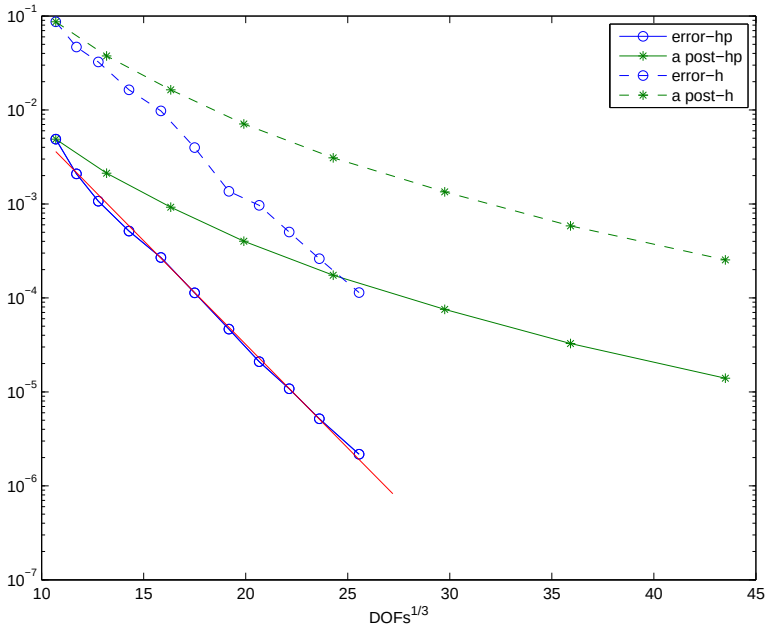

FIGURE 4. Errors and error estimates. Triangle with a hole.

In Figure 6 we plot the relative errors and error estimates for the first two eigenvalues for both the h-adaptive method and hp-adaptive method. For this example we have obtained $\alpha = 0.2453$. In Figures 7 we plot the corresponding values of the effectivity quotient for the hp-adaptive method. We again see exponential convergence for the hp-adaptive method and clearly only polynomial convergence for the h-adaptive method, which is consistent with the theory. In this particular example the gap between the two adaptive methods is very large, which is understandable in view of the fact that the solutions are smooth, and so increasing the order of the elements reduces the error very rapidly.

4.4. **Unit Square with Discontinuous Diffusion Term.** For this Type I problem, Ω is again the unit square with a 1/2-unit square inclusion in its center (see Figure 3). Here $\mathsf{A} = aI$, with

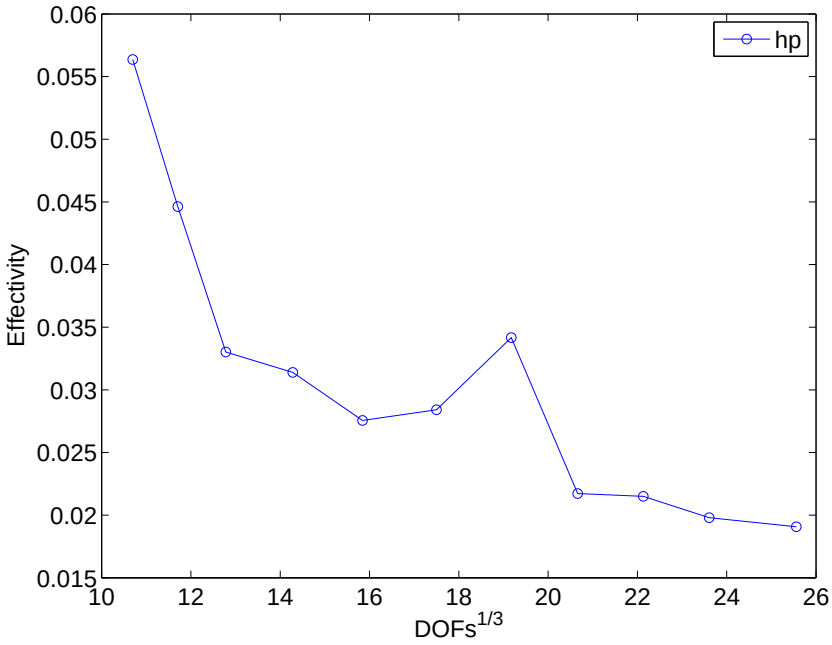

FIGURE 5. Effectivity index. Triangle with a hole.

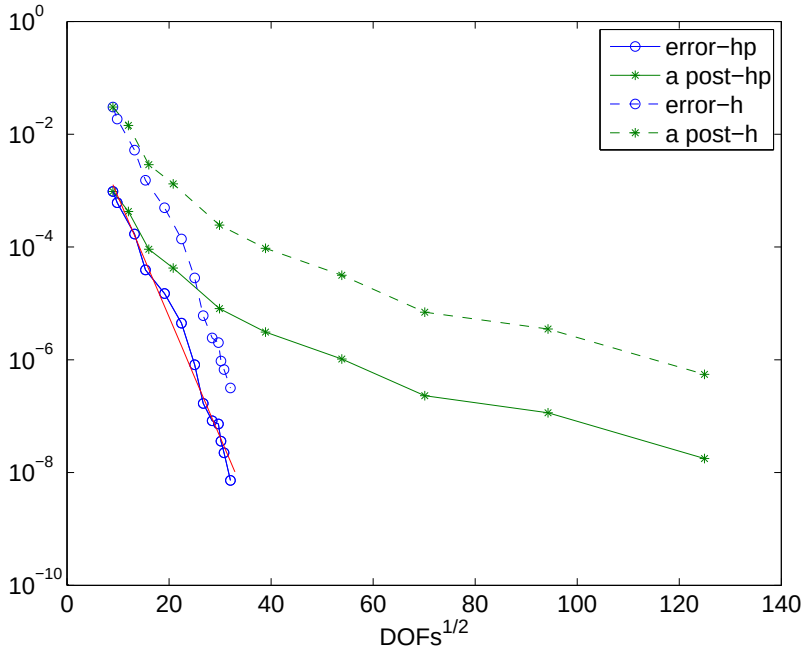

FIGURE 6. Errors and error estimates. Square problem.

$a = 1$ outside the inclusion; and we consider three different values of a inside the inclusion, $a = 10,\ 100,\ 1000$.

In Figures 8, 10 and 12 we plot the total relative errors for the first two eigenvalues, together with the associated error estimates for the three considered cases for both the h-adaptive method

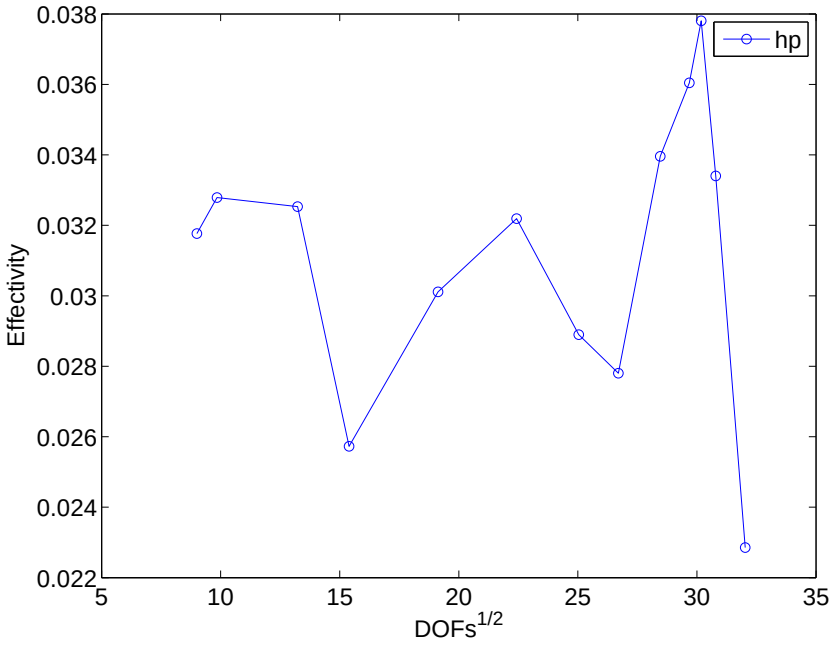

FIGURE 7. Effectivity index. Square problem.

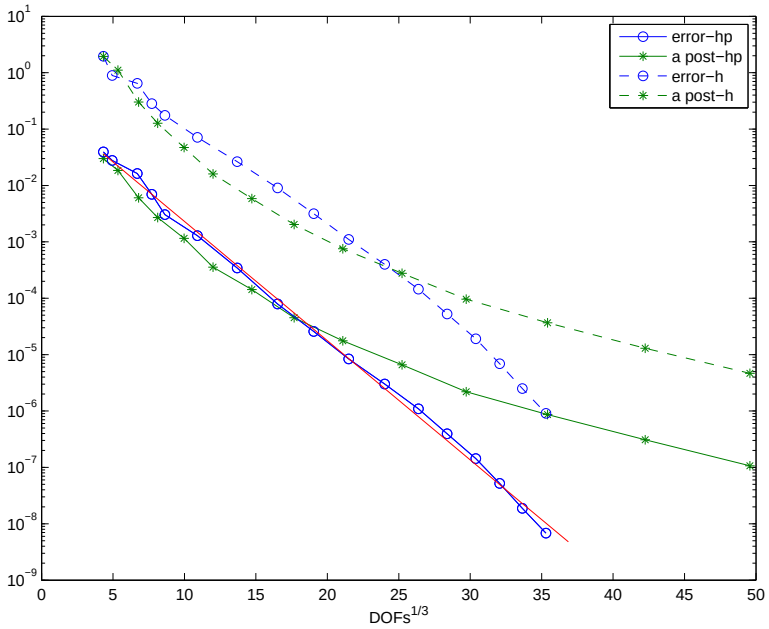

FIGURE 8. Errors and error estimates. Square problem with $a = 10$ inside the inclusion.

and *hp*-adaptive method; and in Figures 9, 11 and 13 we plot the effectivity quotients for the *hp*-adaptive method. It is clear that the convergence is exponential in all cases, and that the error estimator is always robust and as it can be seen the effectivity quotient seems to be independent on the jump in value of the coefficient A. Moreover in Figures 14 and 15 we reported the final meshes and the final distribution of polynomials orders for the cases $a = 10,\ 1000$. As can be seen the

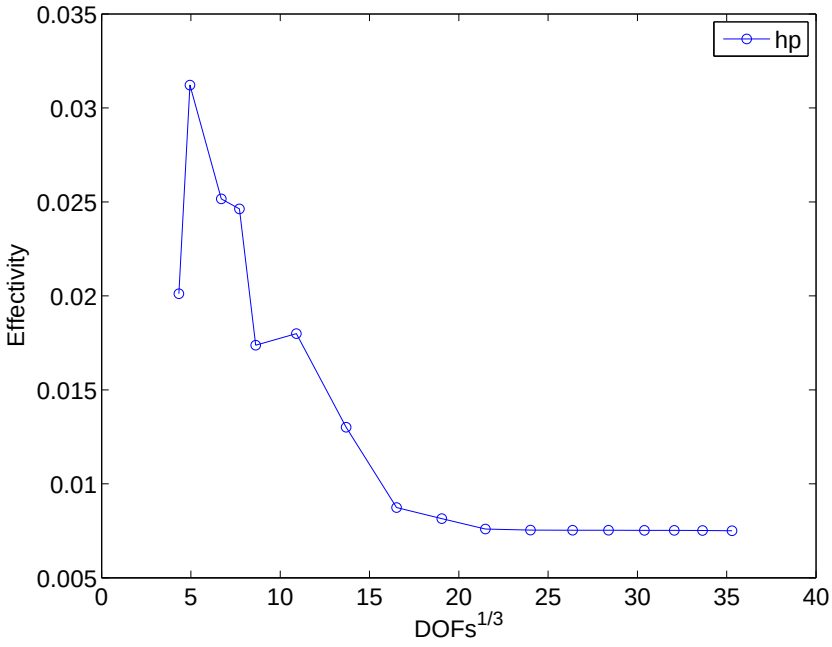

FIGURE 9. Effectivity index. Square problem with $a = 10$ inside the inclusion.

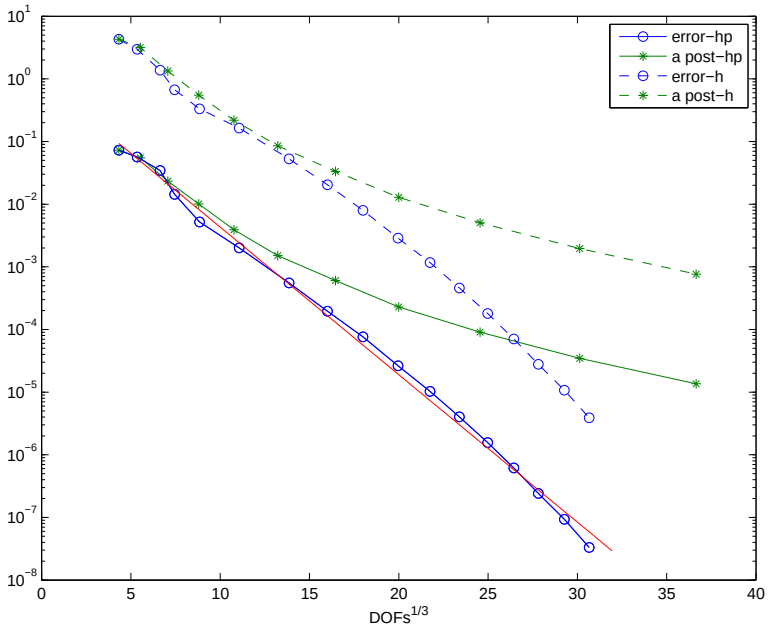

FIGURE 10. Errors and error estimates. Square problem with $a = 100$ inside the inclusion.

adaptive procedure has automatically heavily refined around the corners of the inclusion, where the gradient of the eigenfunctions is expected to be unbounded. For such choices of a we have obtained the following values of α: 0.2435, 0.2711, and 0.2708, respectively. The fact that these do not vary much suggest that our *hp*-adaptive method is robust with respect to jump discontinuities of this sort. The reference values for the first non-zero eigenvalue, which has multiplicity two for

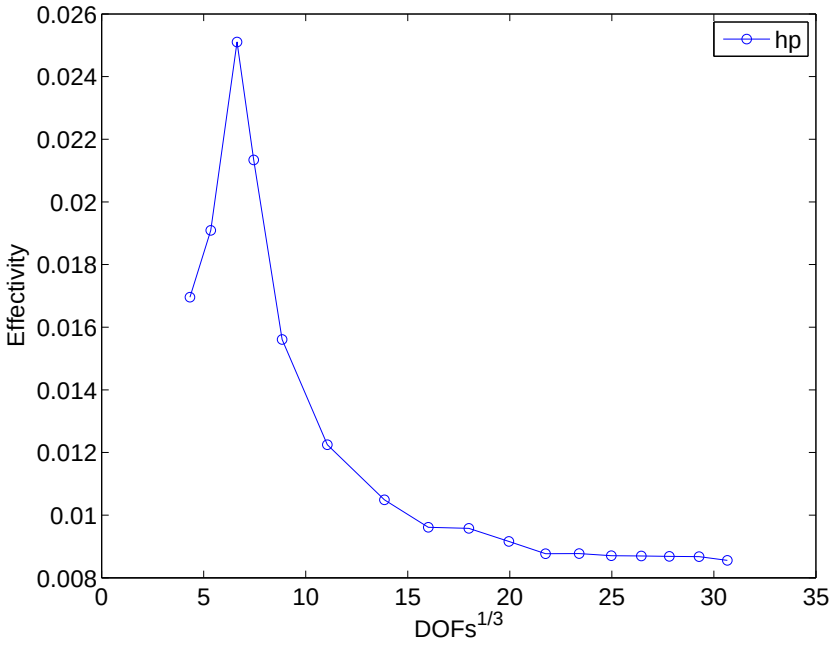

FIGURE 11. Effectivity index. Square problem with $a = 100$ inside the inclusion.

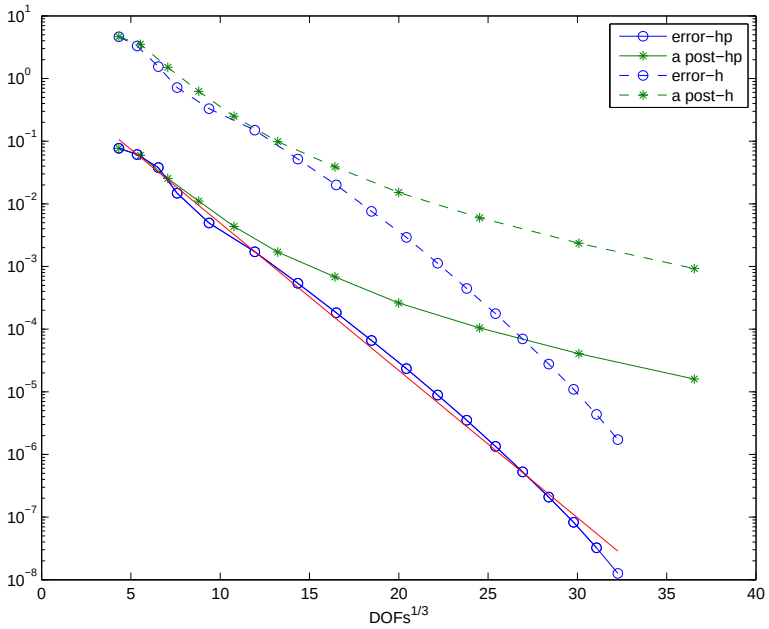

FIGURE 12. Errors and error estimates. Square problem with $a = 1000$ inside the inclusion.

all three cases, for $a = 10,\ 100,\ 1000$ are respectively: 21.332601134 (1e-8), 25.635257891 (1e-8) and 26.165986004 (1e-8).

4.5. **Kellogg Problem.** A class of Type I problems for which the singularities can be extremely strong have been carefully considered by Kellogg [23] and others for boundary value problems. Here

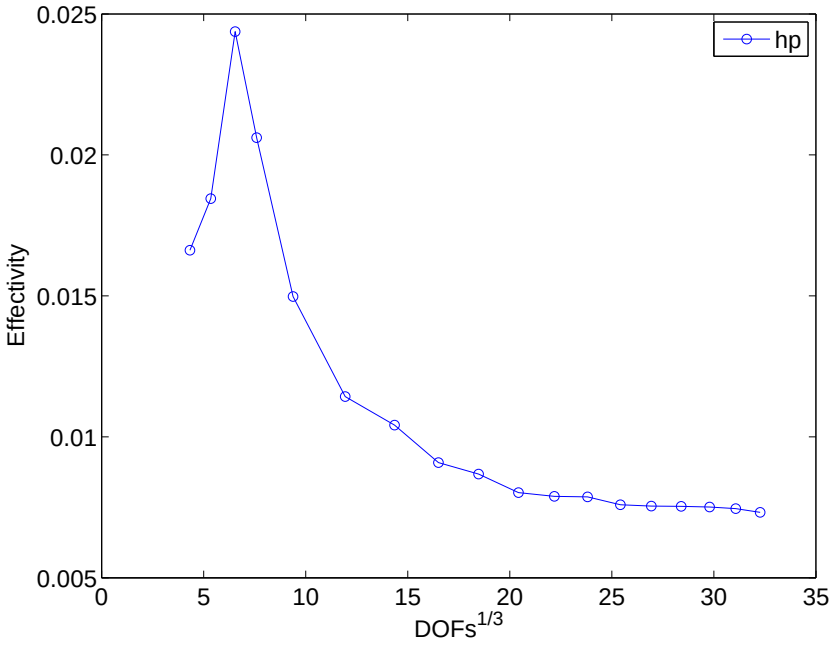

FIGURE 13. Effectivity index. Square problem with $a = 1000$ inside the inclusion.

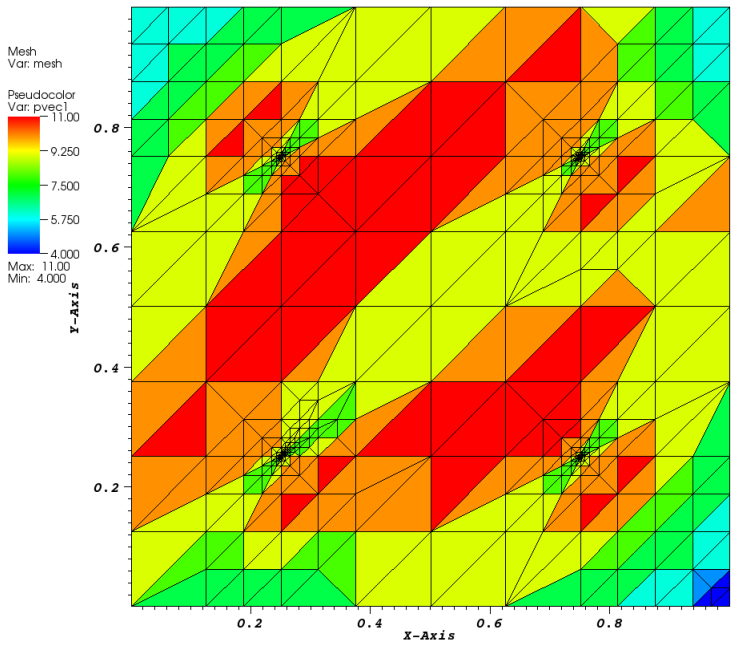

FIGURE 14. Mesh and order of polynomials. Square problem with $a = 10$ inside the inclusion.

we take Ω as the unit square, partitioned into regions $\mathcal{M}_1$ and $\mathcal{M}_2$ as in Figure 16. We take $\mathsf{A} = aI$,

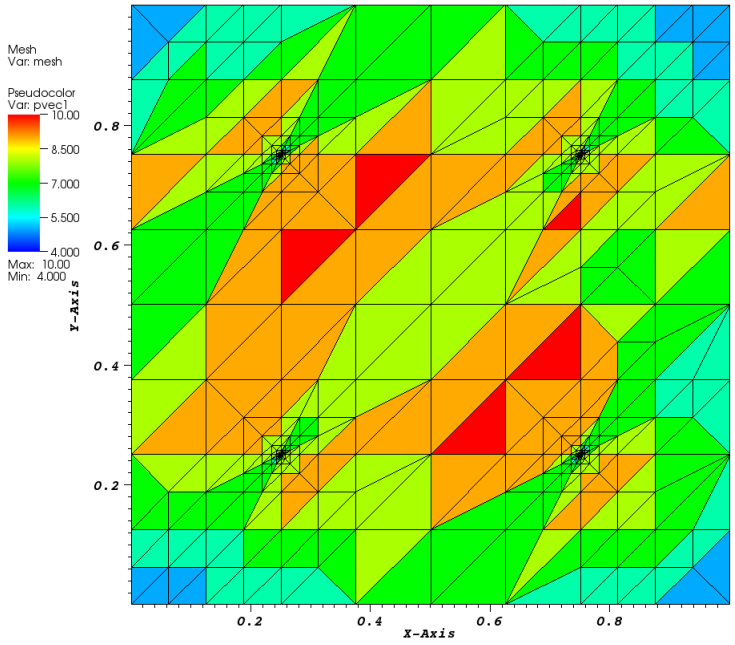

FIGURE 15. Mesh and order of polynomials. Square problem with $a = 1000$ inside the inclusion.

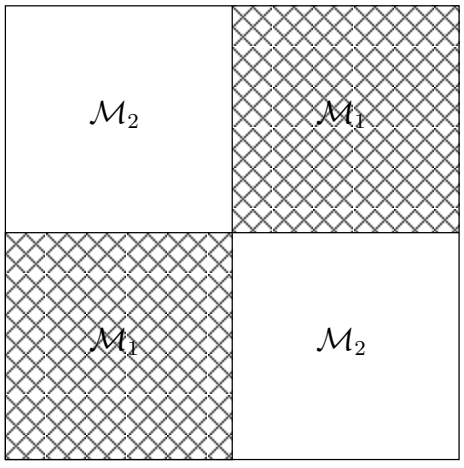

FIGURE 16. A modification of the touching squares example of M. Dauge.

with $a = 1$ in $\mathcal{M}_2$, and two different values of a in $\mathcal{M}_1$: 5 and 10. Since the exact eigenvalues are not available, we computed the following three reference values for the first three eigenvalues different from zero: for $a = 5$ we have 16.683094083 (1e-8), 19.2021789 (1e-6), 27.363024736 (1e-8); and for $a = 10$ we have 18.135407487 (1e-8), 25.001324 (1e-5), 28.148296784 (1e-8). In Figure 17 we show a plot of the eigenfunction of the second eigenvalue different from zero for the case $a = 10$, which clearly exhibits a very strong singularity at the center of the domain. The reference values for

the second eigenvalues for both values of a are very hard to compute because of such singularities. The presence of these strong singularities has been noticed by the adaptive algorithm, as can be seen in Figure 22 where the region in the center of the domain has been heavily refined.

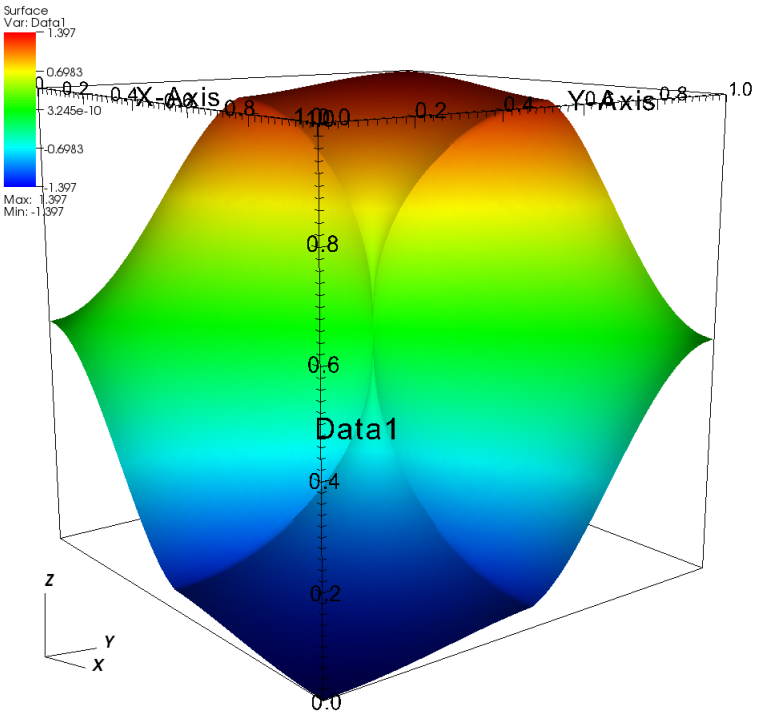

FIGURE 17. Eigenfunction of the second eigenvalue different from zero for $a = 10$.

Convergence and effectivity plots for the first three non-zero eigenvalues are given in Figures 18-19 for $a = 5$, and in Figures 20-21 for $a = 10$. When $a = 5$ we obtain the rate $\alpha = 0.3333$, and when $a = 10$ we obtain $\alpha = 0.2542$.

4.6. **Periodic Problem with Discontinuous Diffusion Term.** We consider Type II (periodic) problem with $\kappa = (0, 0)$, where the "primitive cell" is the unit square with a square inclusion, precisely as in subsection 4.4. As before, we let $\mathsf{A} = aI$, where $a = 1$ outside the inclusion and $a = 10$ or $a = 100$ inside the inclusion.

In Figures 23 and 25 we plot the total relative errors for the first two eigenvalues, together with the associated error estimates for the two considered cases and for both the h-adaptive method and hp-adaptive method; and in Figure 24 and 26 we plot the effectivity quotients only for the hp-adaptive method. It is clear that the convergence is exponential in both cases using the hp-adaptive method, and that the error estimator is robust—the vales of α, 0.1752 and 0.1957, respectively, are pretty close together. The reference values for the first non-zero eigenvalue for $a = 10,\ 100$ are respectively: 49.644578674 (2e-8) and 51.146497655 (5e-8).

4.7. **Photonic Crystal Example.** As last examples we consider the sesquilinear form B_κ in (2.3), which has applications in nano-optics. For each value of κ the spectrum of B_κ is discrete. At the same time the eigenvalues form continuous bands when they are seen as function in κ.

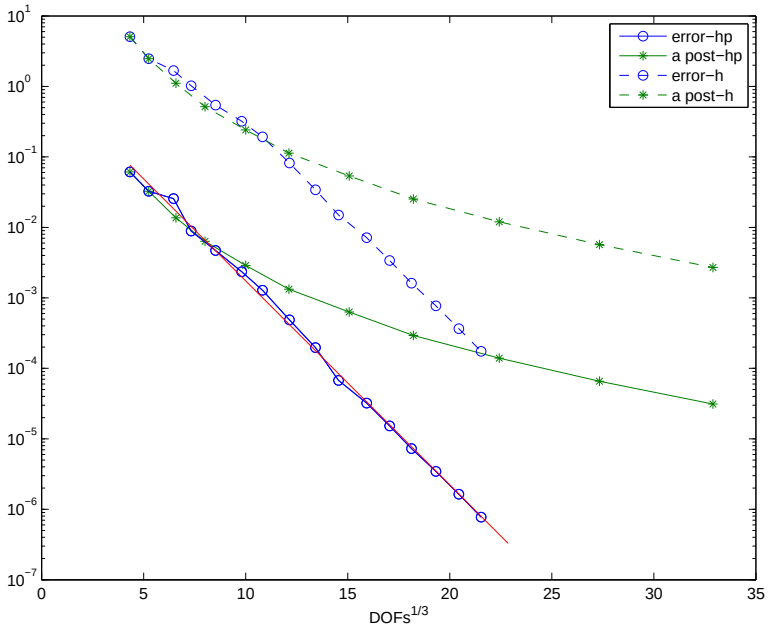

FIGURE 18. Errors and error estimates. Kellogg problem, $a = 5$ in $\mathcal{M}_1$.

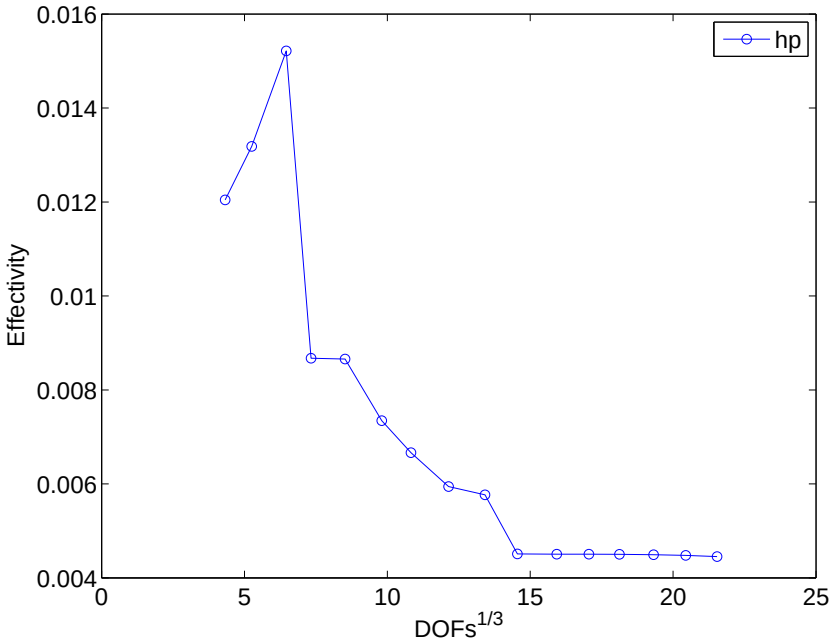

FIGURE 19. Effectivity index. Kellogg problem, $a = 5$ in $\mathcal{M}_1$.

A typical example of such band structure for a primitive cell with a single inclusion is reported in Figure 27(a). In order to produce accurately the band structure of the crystal it is sufficient to compute the eigenvalues of B_κ for the values of κ in the reduced Brillouin zone, also called irreducible Brillouin zone. For sake of clarity we just consider the values of κ on the border of the reduced Brillouin zone, which has been parametrized in r. As can be seen in Figure 27(b) the

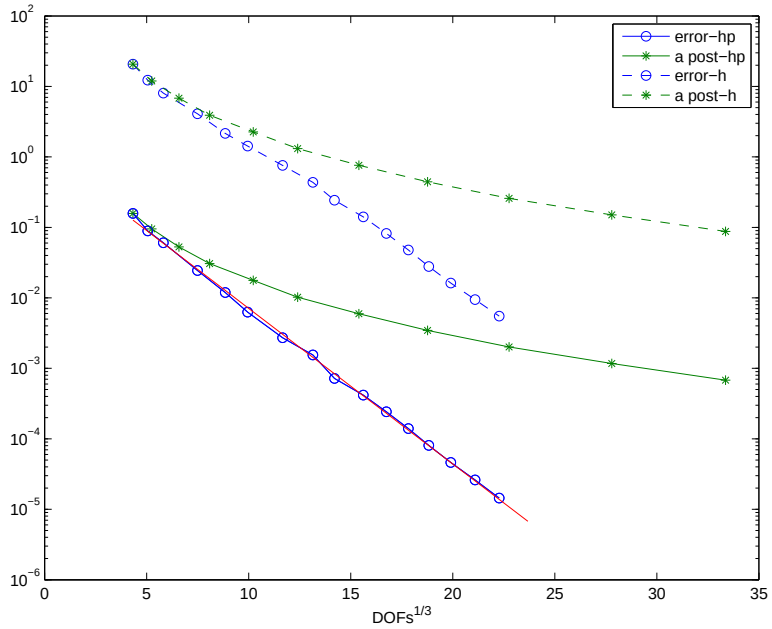

FIGURE 20. Errors and error estimates. Kellogg problem, $a = 10$ in $\mathcal{M}_1$.

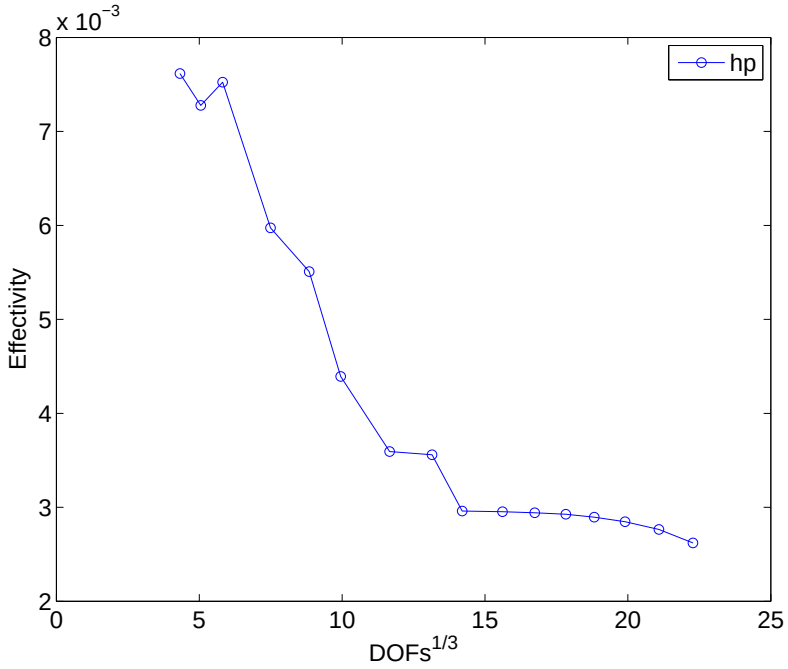

FIGURE 21. Effectivity index. Kellogg problem, $a = 10$ in $\mathcal{M}_1$.

minimum and the maximum of each function $\lambda_j(\kappa)$ delimits a band of the spectrum, and between bands gaps can sometimes be found. In this example there appears to be a gap between the first and the second band.

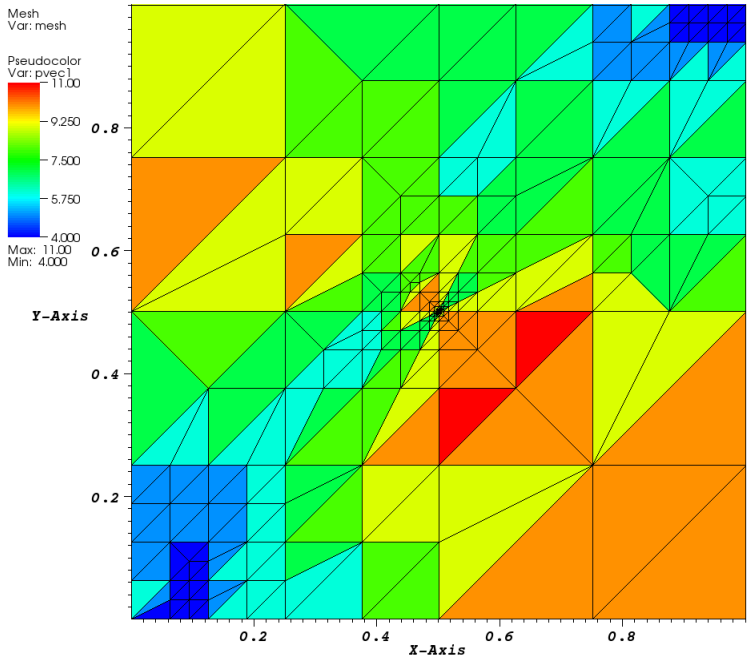

FIGURE 22. Mesh and order of polynomials. Kellogg problem, $a = 10$ in $\mathcal{M}_1$.

A more interesting case is when a compact defect in the periodic structure may create localized eigenvalues in the gaps that correspond to trapped modes. As an example computing the band structure of the supercell we obtain Figure 28(b), where a new narrow band is present in the first gap.

For our examples the domain is the same as in Section 4.4, again with $\mathsf{A} = aI$, and $a = 1$ outside the inclusion. Inside the inclusion, we take $a = 10$. Initially we consider two values for the quasi-momentum κ: either $(1, 1)$ or $(2\pi, 0)$. For the first of these, operator is positive definite. For the second, it is semi-definite, with $\mathrm{Ker}(B) \cap V = \{0\}$.

In Figures 29 and 31 we plot the relative errors for the second eigenvalues, together with the associated error estimates for the two considered cases and for both the h-adaptive method and hp-adaptive method; and in Figures 30 and 32 we plot the effectivity quotients only for the hp-adaptive method. It is clear that the hp-adaptive method converges faster than the h-adaptive method and for the former the values of α are 0.2194 and 0.1851. The reference values for the eigenvalues in the second band for $\kappa = (1, 1)$, $(2\pi, 0)$ are respectively: 39.745072858 (1e-8) and 49.644578756 (1e-8).

Finally in Figures 33 and 34 we report the convergence of the error for the eigenvalue in the second band for values of $\kappa = (2\pi - s, s)$ for the following values of s: 0, 0.1, 0.01, 10e-4, 10e-8, 10e-16. For all values of s, except for $s = 0$, the corresponding problems have trivial kernels. As can be seen the convergence plots are all very similar, and moreover the effectivity indexes are all in the same range of values for all s. This seems to suggest that the error estimator ε_i is robust in κ as κ approaches values for which the problem becomes semi-definite.

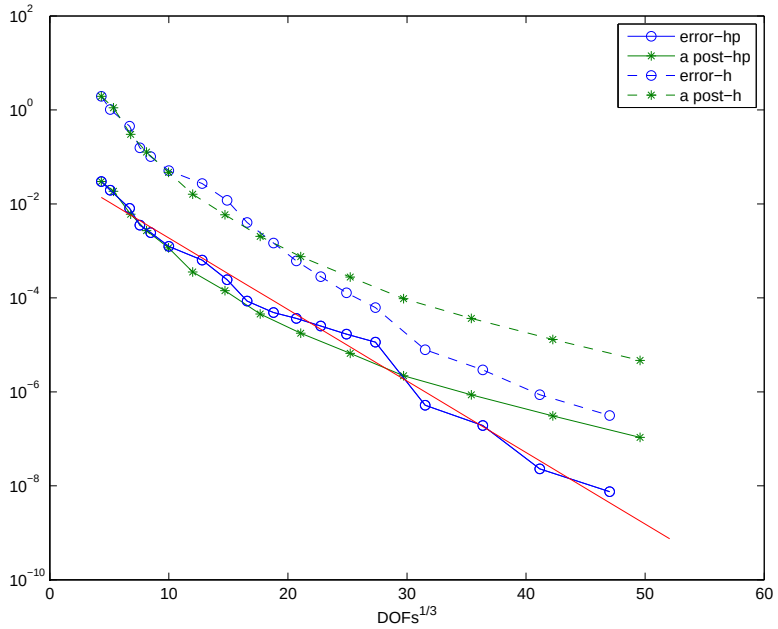

FIGURE 23. Errors and error estimates. Periodic square problem, $a = 10$ inside the inclusion.

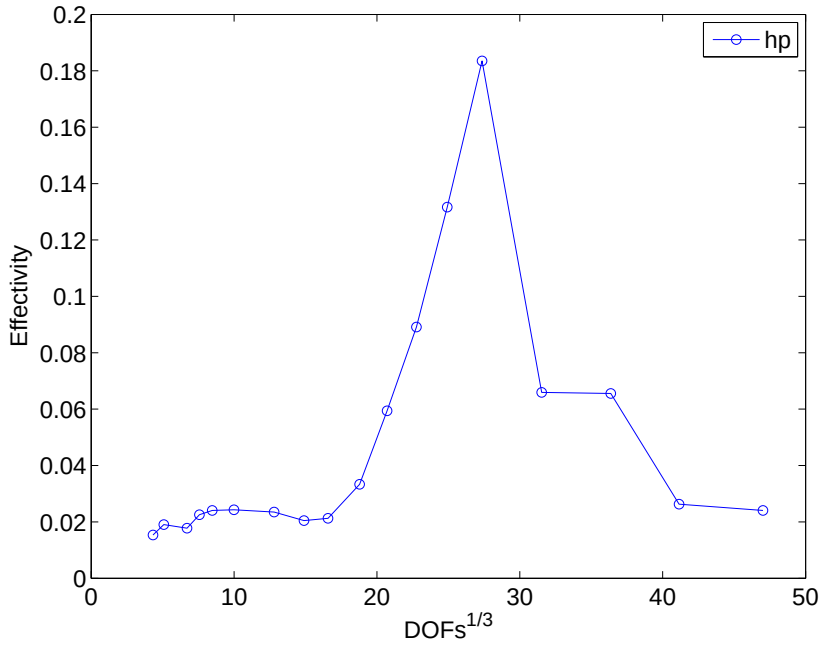

FIGURE 24. Effectivity index. Periodic square problem, $a = 10$ inside the inclusion.

5. Concluding Remarks

The *hp*-adaptive approach discussed here and in the companion paper [17] provides a robust error theory as well as an efficient, high-order method for eigenvalue and invariant subspace computations. This robustness in theory and practice is with respect to singularities in the eigenfunctions arising

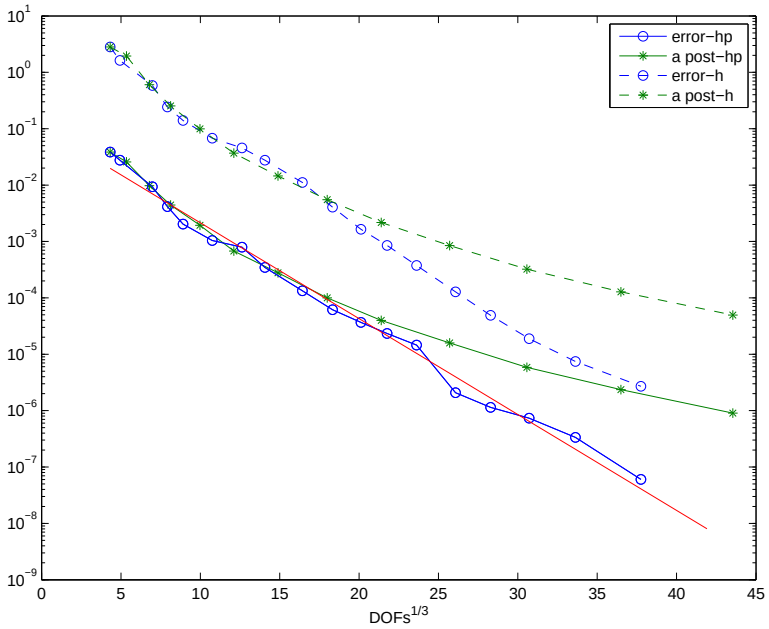

FIGURE 25. Errors and error estimates. Periodic square problem, $a = 100$ inside the inclusion.

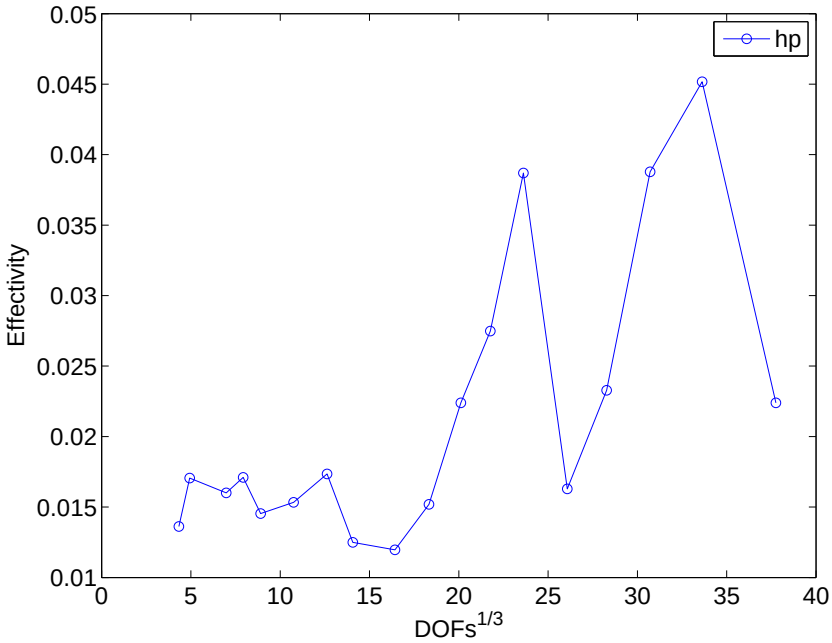

FIGURE 26. Effectivity index. Periodic square problem, $a = 100$ inside the inclusion.

from non-convex geometries and discontinuities in the coefficients differential operator, as well as degenerate eigenvalues. Extensive numerical experiments on a variety of challenging problems which represent many of the difficulties present in realistic applications demonstrate the viability of this general approach.

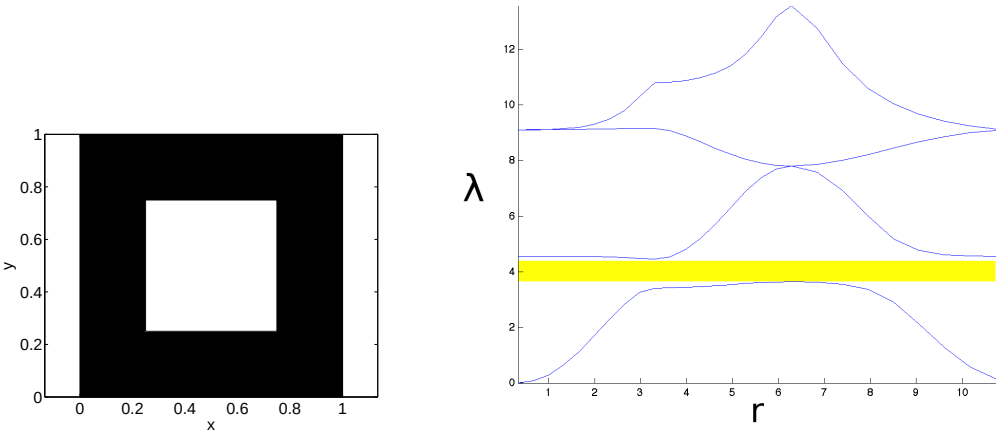

(a) (b)

FIGURE 27. (a) Structure of the primitive cell. (b) Band structure of the spectrum for the periodic crystal with primitive cell as in (a). The first gap has been highlighted in yellow.

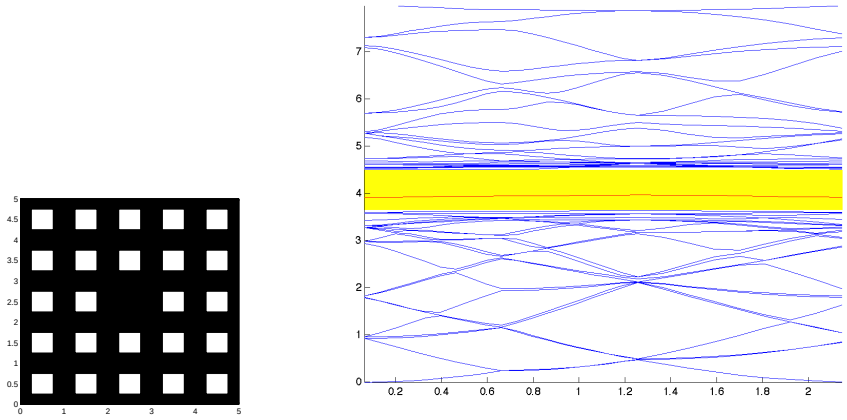

(a) (b)

FIGURE 28. (a) Structure of the supercell with a defect in the center. (b) Band structure of the spectrum for the supercell in (a). The first gap has been highlighted in yellow and the newly created trapped band in red.

We point out that, although we have chosen the *a posteriori* error estimates of Melenk and Wolmuth [25] in our practical implementation for both "global" error estimates as well as for selecting elements for refinement, any number of *hp a posteriori* error estimates for boundary value problems can be readily "plugged into" our framework with very little change in theory or implementation. For example, one might use a recovery-based approach such as that in [10] or higher-order versions of either [26] or [8]. For each of these approaches an approximate error function is obtained, which gives greater flexibility in how we use it to estimate approximation defects. As can be seen from their definition (via the Courant-Fischer Theorem), the approximation defects

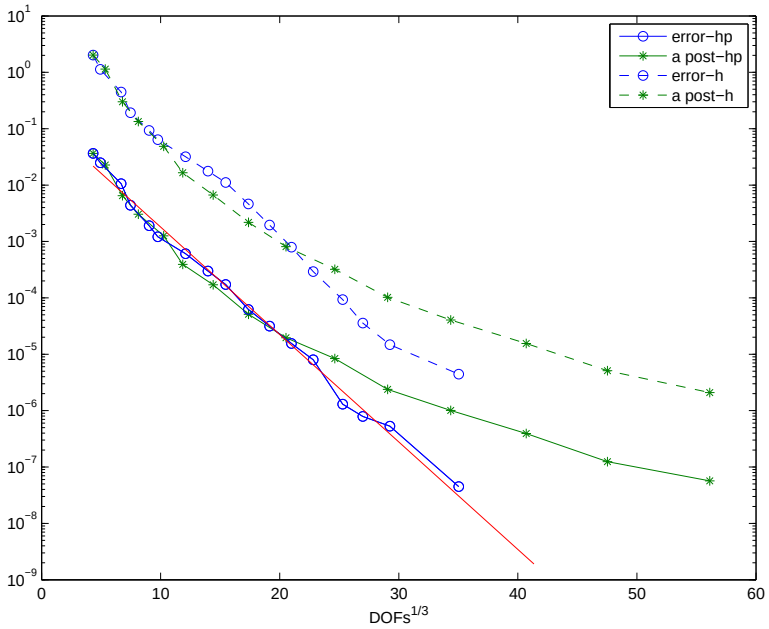

FIGURE 29. Errors and error estimates for $\kappa = (1, 1)$.

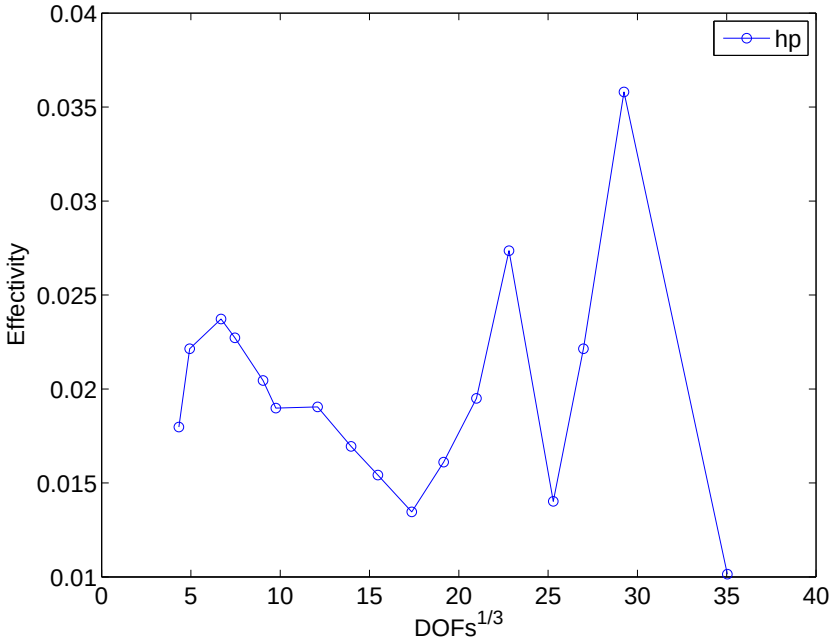

FIGURE 30. Effectivity index for $\kappa = (1, 1)$.

are themselves the solutions of a small $(m \times m)$ generalized eigenvalue problem—this is discussed explicitly in [8]. The present approach is based on approximating only the diagonal of the associated $m \times m$ matrices, and this is all that can be reliably done with residual-based error estimates. With approximate error functions, however, the off-diagonals of these matrices can also be approximated,

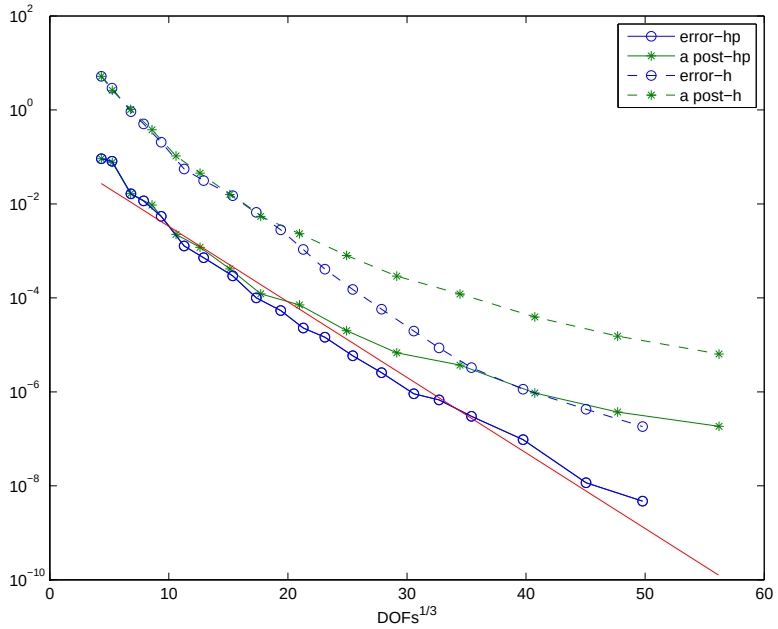

FIGURE 31. Errors and error estimates for $\kappa = (2\pi, 0)$.

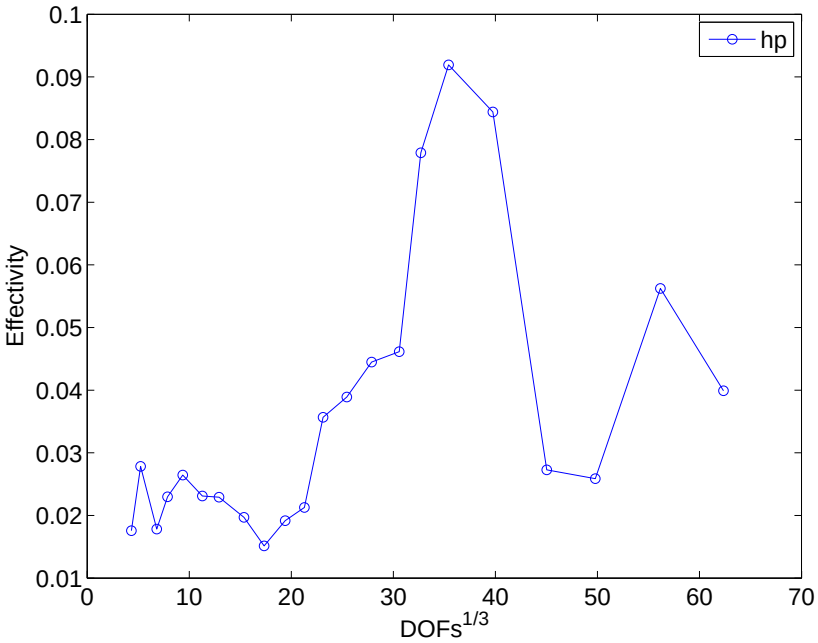

FIGURE 32. Effectivity index for $\kappa = (2\pi, 0)$.

which permits greater effectivity quotients in the estimates, as was seen in [8] for low-order elements and h-refinement.

Another issue which we plan to address in future work is related to the choice of h- or p-refinement, a topic which still seems unsettled even for boundary value problems. This choice was made here by estimating local analyticity in the manner of [14]. The complete disconnect between

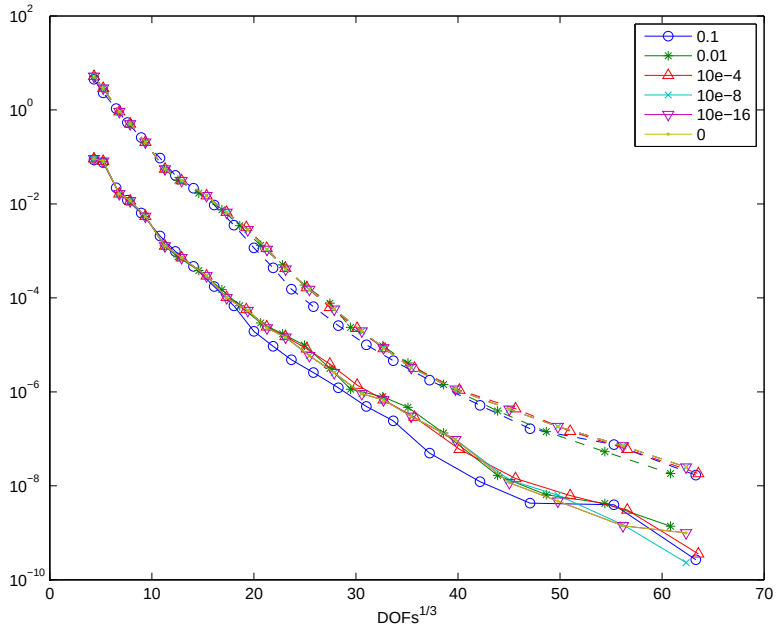

FIGURE 33. Errors and error estimates for $\kappa = (2\pi - s, s)$.

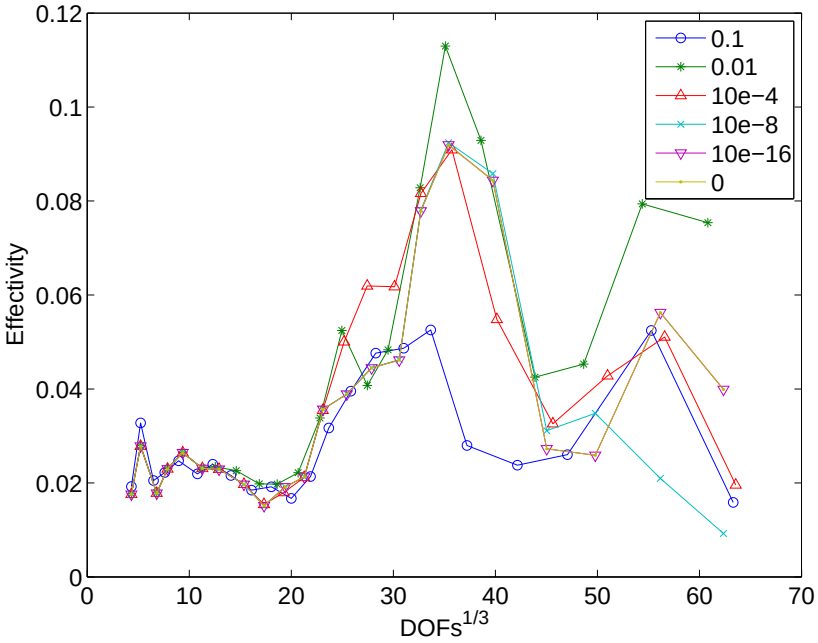

FIGURE 34. Effectivity indexes for $\kappa = (2\pi - s, s)$.

the methods used for selecting elements for refinement and the choice how they should be refined is philosophically unappealing, so further efforts will be devoted to developing, if possible, marking and refinement strategies which are more closely related to each other. Any of the "approximate error function" techniques mentioned above make such a goal seem feasible. In particular, since *hp*

finite element spaces naturally have a hierarchical structure, an *hp*-variant of the hierarchical basis approach from [8] is appealing in this regard, and will be pursued further.

Acknowledgement

L. G. was supported by the grant: "Spectral decompositions – numerical methods and applications", Grant Nr. 037-0372783-2750 of the Croatian MZOS. We would like to thanks Paul Houston and Edward Hall for kind support and very useful discussions.

References

[1] G. Acosta, T. Apel, R. G. Durán, and A. L. Lombardi. Anisotropic error estimates for an interpolant defined via moments. *Computing*, 82:1–9, April 2008.

[2] P. Amestoy, I. Duff, and J.-Y. L'Excellent. Multifrontal parallel distributed symmetric and unsymmetric solvers. *Computer Methods in Applied Mechanics and Engineering*, 184(2–4):501–520, 2000.

[3] H. Ammari, Y. Capdeboscq, H. Kang, and A. Kozhemyak. Mathematical models and reconstruction methods in magneto-acoustic imaging. *European J. Appl. Math.*, 20(3):303–317, 2009.

[4] H. Ammari, H. Kang, E. Kim, and H. Lee. Vibration testing for anomaly detection. *Math. Methods Appl. Sci.*, 32(7):863–874, 2009.

[5] H. Ammari, H. Kang, and H. Lee. Asymptotic analysis of high-contrast phononic crystals and a criterion for the band-gap opening. *Arch. Ration. Mech. Anal.*, 193(3):679–714, 2009.

[6] M. G. Armentano, C. Padra, R. Rodríguez, and M. Scheble. An *hp* finite element adaptive scheme to solve the Laplace model for fluid-solid vibrations. *Comput. Methods Appl. Mech. Engrg.*, 200(1-4):178–188, 2011.

[7] I. Babuška and B. Q. Guo. The h-p version of the finite element method for domains with curved boundaries. *SIAM Journal on Numerical Analysis*, 25(4):837–861, 1988. ArticleType: research-article / Full publication date: Aug., 1988 / Copyright 1988 Society for Industrial and Applied Mathematics.

[8] R. Bank, L. Grubišić, and J. S. Ovall. A framework for robust eigenvalue and eigenvector error estimation and ritz value convergence enhancement. *submitted*, MPI MSI Leipzig preprint 42/2010, 2010.

[9] R. E. Bank. Hierarchical bases and the finite element method. In *Acta numerica, 1996*, volume 5 of *Acta Numer.*, pages 1–43. Cambridge Univ. Press, Cambridge, 1996.

[10] R. E. Bank, J. Xu, and B. Zheng. Superconvergent derivative recovery for lagrange triangular elements of degree p on unstructured grids. *SIAM J. Numer. Anal.*, submitted.

[11] T. Betcke and L. N. Trefethen. Reviving the method of particular solutions. *SIAM Rev.*, 47(3):469–491 (electronic), 2005.

[12] M. Blumenfeld. Interface-Eigenwertprobleme auf polaren Gittern. *Z. Angew. Math. Mech.*, 64(5):266–268, 1984.

[13] M. Blumenfeld. The regularity of interface-problems on corner-regions. In *Singularities and constructive methods for their treatment (Oberwolfach, 1983)*, volume 1121 of *Lecture Notes in Math.*, pages 38–54. Springer, Berlin, 1985.

[14] T. Eibner and J. Melenk. An adaptive strategy for hp-fem based on testing for analyticity. *Comp. Mech.*, 39:575–595, 2007.

[15] S. C. Eisenstat. On the rate of convergence of the Bergman-Vekua method for the numerical solution of elliptic boundary value problems. *SIAM J. Numer. Anal.*, 11:654–680, 1974.

[16] S. Giani and I. Graham. Adaptive finite element methods for computing band gaps in photonic crystals. *Numerische Mathematik*, to appear.

[17] S. Giani, L. Grubišić, and J. Ovall. Reliable *a-posteriori* error estimators for *hp*-adaptive finite element approximations of eigenvalue/eigenvector problems. *Nothingam ePrints*, http://eprints.nottingham.ac.uk/, 2011.

[18] S. Giani, L. Grubišić, and J. Ovall. Benchmark results for testing adaptive finite element eigenvalue procedures. *Applied Numerical Mathematics*, 62(2):121–140, 2012.

[19] L. Grubišić. On eigenvalue and eigenvector estimates for nonnegative definite operators. *SIAM J. Matrix Anal. Appl.*, 28(4):1097–1125 (electronic), 2006.

[20] L. Grubišić. Relative convergence estimates for the spectral asymptotic in the large coupling limit. *Integral Equations Operator Theory*, 65(1):51–81, 2009.

[21] L. Grubišić and J. S. Ovall. On estimators for eigenvalue/eigenvector approximations. *Math. Comp.*, 78:739–770, 2009.

[22] P. Houston and E. Süli. A note on the design of hp-adaptive finite element methods for elliptic partial differential equations. *Computer Methods in Applied Mechanics and Engineering*, 194(2-5):229–243, Feb. 2005.

[23] R. B. Kellogg. On the Poisson equation with intersecting interfaces. *Applicable Anal.*, 4:101–129, 1974/75. Collection of articles dedicated to Nikolai Ivanovich Muskhelishvili.

[24] B. J. McCartin. Eigenstructure of the equilateral triangle. II. The Neumann problem. *Math. Probl. Eng.*, 8(6):517–539, 2002.
[25] J. M. Melenk and B. I. Wohlmuth. On residual-based a posteriori error estimation in *hp*-FEM. *Adv. Comput. Math.*, 15(1-4):311–331 (2002), 2001. A posteriori error estimation and adaptive computational methods.
[26] A. Naga and Z. Zhang. Function value recovery and its application in eigenvalue problems. *SIAM J. Numer. Anal.*, to appear.
[27] J. Weidmann. Stetige Abhängigkeit der Eigenwerte und Eigenfunktionen elliptischer Differentialoperatoren vom Gebiet. *Math. Scand.*, 54(1):51–69, 1984.

School of Mathematical Sciences University of Nottingham , University Park, Nottingham, NG7 2RD, United Kingdom
E-mail address: stefano.giani@nottingham.ac.uk

University of Zagreb, Department of Mathematics, Bijenička 30, 10000 Zagreb, Croatia
E-mail address: luka.grubisic@math.hr

University of Kentucky, Department of Mathematics, Patterson Office Tower 761, Lexington, KY 40506-0027, USA
E-mail address: jovall@ms.uky.edu